

Supplementary Materials: Optical Characterization of Gadolinium Fluoride Films by Universal Dispersion Model

Daniel Franta ^{1,*}, Jiří Vohánka ¹, Jan Dvořák ¹, Pavel Franta ¹, Ivan Ohlídal ¹, Petr Klapetek ², Jaromír Březina ³ and David Škoda ³

1. Experimental data

In Table S1 the complete set of the experimental data used for heterogeneous data processing is listed together with their respective ranges and angles of incidence. Links to the concrete figures are included. In those figures the best fit is presented with the experimental data points. All experimental points shown in the graphs were fitted except for the degree of polarization P for the ellipsometric data. The degree of polarization is a quantity calculated as follows

$$P = \sqrt{I_s^2 + I_c^2 + I_n^2}.$$

Table S1. List of data sets used for optical characterization

	instrument	quantity	mode	range	figures
1	Woollam IR-VASE	I_s, I_c, I_n	front	$250\text{--}6000\text{ cm}^{-1}, 55\text{--}75^\circ$	S1, S2, S3, S4, S5
2	Woollam IR-VASE	I_s, I_c, I_n	back	$250\text{--}6000\text{ cm}^{-1}, 55\text{--}75^\circ$	S6, S7, S8, S9, S10
3	Woollam IR-VASE	$\Delta I_s, \Delta I_c, \Delta I_n$	difference	$250\text{--}6000\text{ cm}^{-1}, 55\text{--}75^\circ$	S11, S12, S13, S14, S15
4	Bruker Vertex 80v	R^f/R^b	relative	$70\text{--}680\text{ cm}^{-1}, 6^\circ$	S16, S17, S18, S19, S20
5	Bruker Vertex 80v	R	front	$70\text{--}680\text{ cm}^{-1}, 6^\circ$	S16, S17, S18, S19, S20
6	Bruker Vertex 80v	R	back	$70\text{--}680\text{ cm}^{-1}, 6^\circ$	S16, S17, S18, S19, S20
7	Bruker Vertex 80v	T		$70\text{--}680\text{ cm}^{-1}, 0^\circ$	S16, S17, S18, S19, S20
8	Bruker Vertex 80v	R^f/R^b	relative	$370\text{--}7500\text{ cm}^{-1}, 6^\circ$	S21, S22, S23, S24, S25
9	Bruker Vertex 80v	R	front	$370\text{--}7500\text{ cm}^{-1}, 6^\circ$	S21, S22, S23, S24, S25
10	Bruker Vertex 80v	R	back	$370\text{--}7500\text{ cm}^{-1}, 6^\circ$	S21, S22, S23, S24, S25
11	Bruker Vertex 80v	T		$370\text{--}7500\text{ cm}^{-1}, 0^\circ$	S21, S22, S23, S24, S25
12	Horiba Jobin Yvon UVISEL	I_s, I_c, I_n	front	$0.6\text{--}6.5\text{ eV}, 55\text{--}75^\circ$	S27, S28, S29, S30, S31
13	Horiba Jobin Yvon UVISEL	I_s, I_c, I_n	back	$1.5\text{--}6.5\text{ eV}, 65^\circ$	S32
14	Perkin Elmer Lambda 1050	R^f/R^b	relative	$187\text{--}860\text{ nm}, 6^\circ$	S33
15	Perkin Elmer Lambda 1050	R	front	$187\text{--}860\text{ nm}, 6^\circ$	S34
16	McPherson UUVAS 1000	R	front	$120\text{--}320\text{ nm}, 10^\circ$	S34

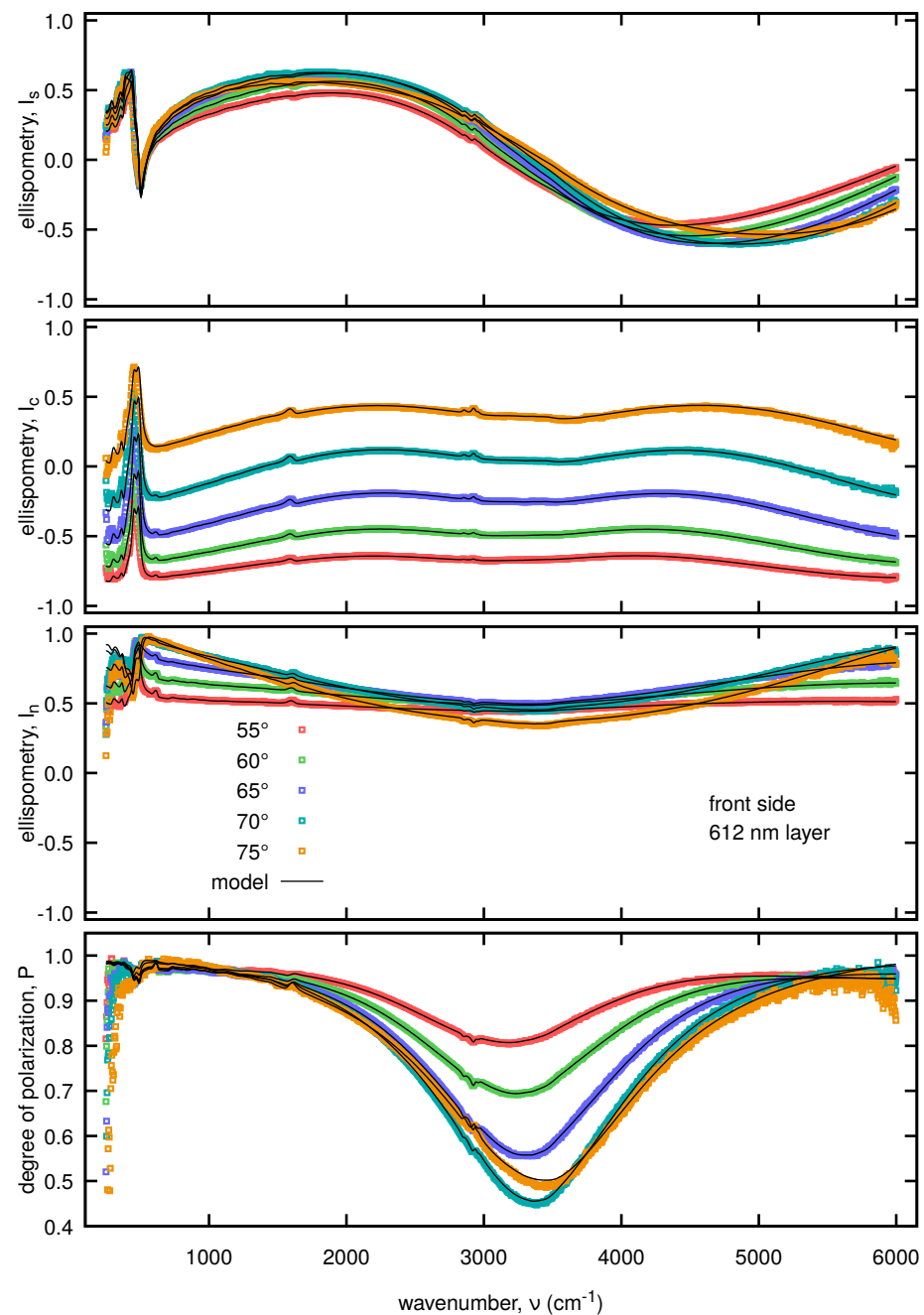


Figure S1. Spectral dependencies of the generalized ellipsometric parameters displayed for the 612 nm thick film #1 (measured from the front side).

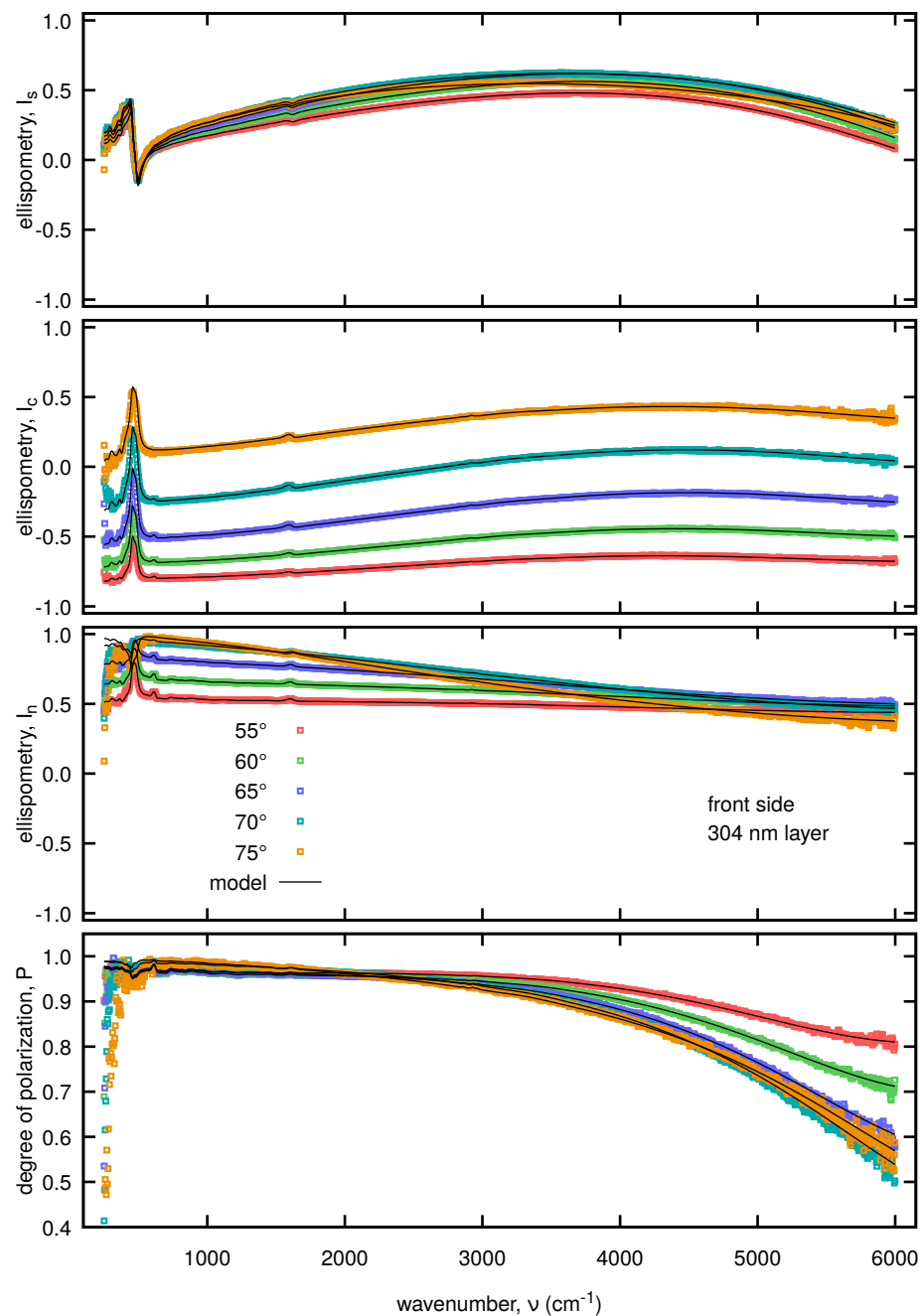


Figure S2. Spectral dependencies of the generalized ellipsometric parameters displayed for the 304 nm thick film #2 (measured from the front side).

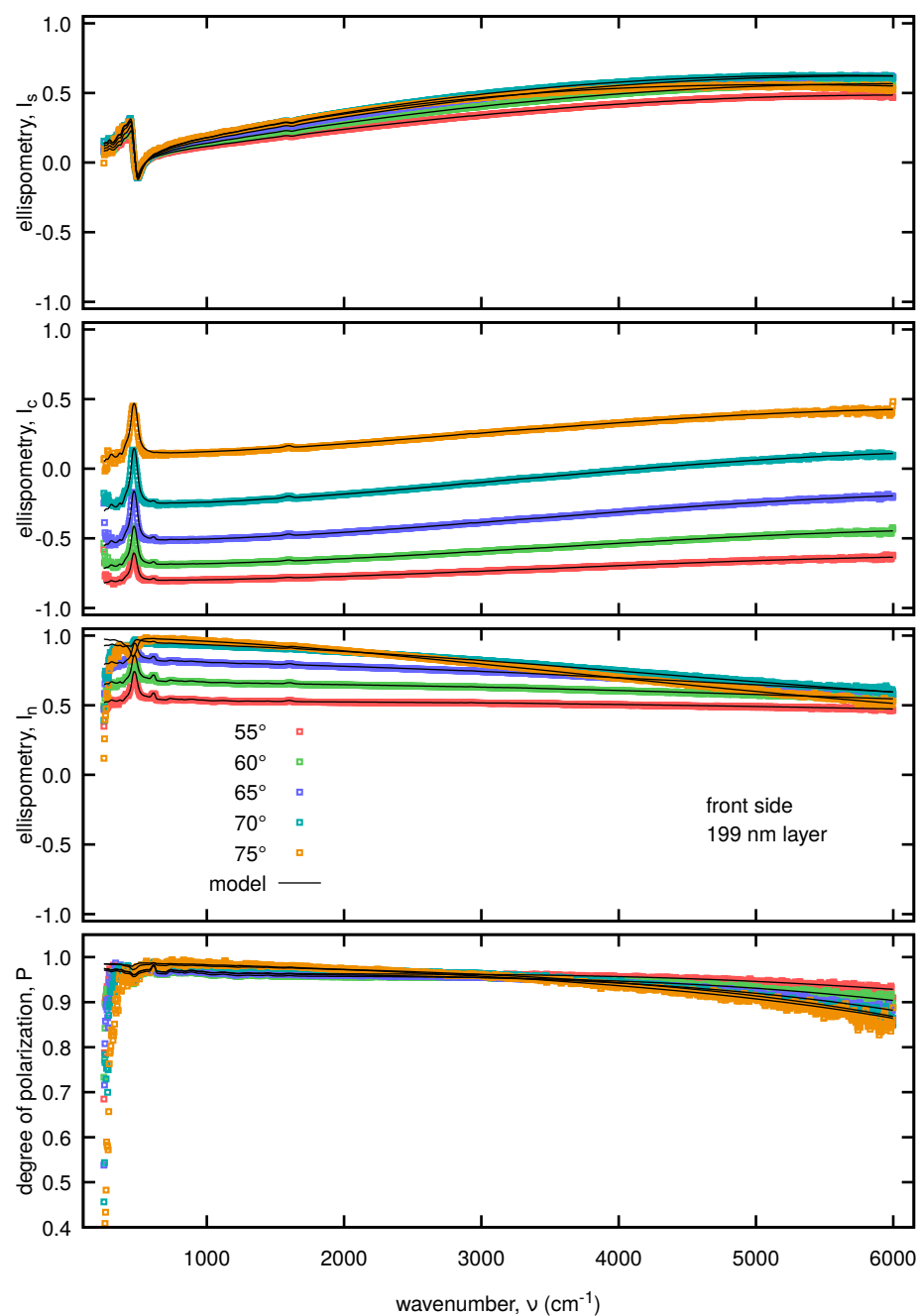


Figure S3. Spectral dependencies of the generalized ellipsometric parameters displayed for the 199 nm thick film #3 (measured from the front side).

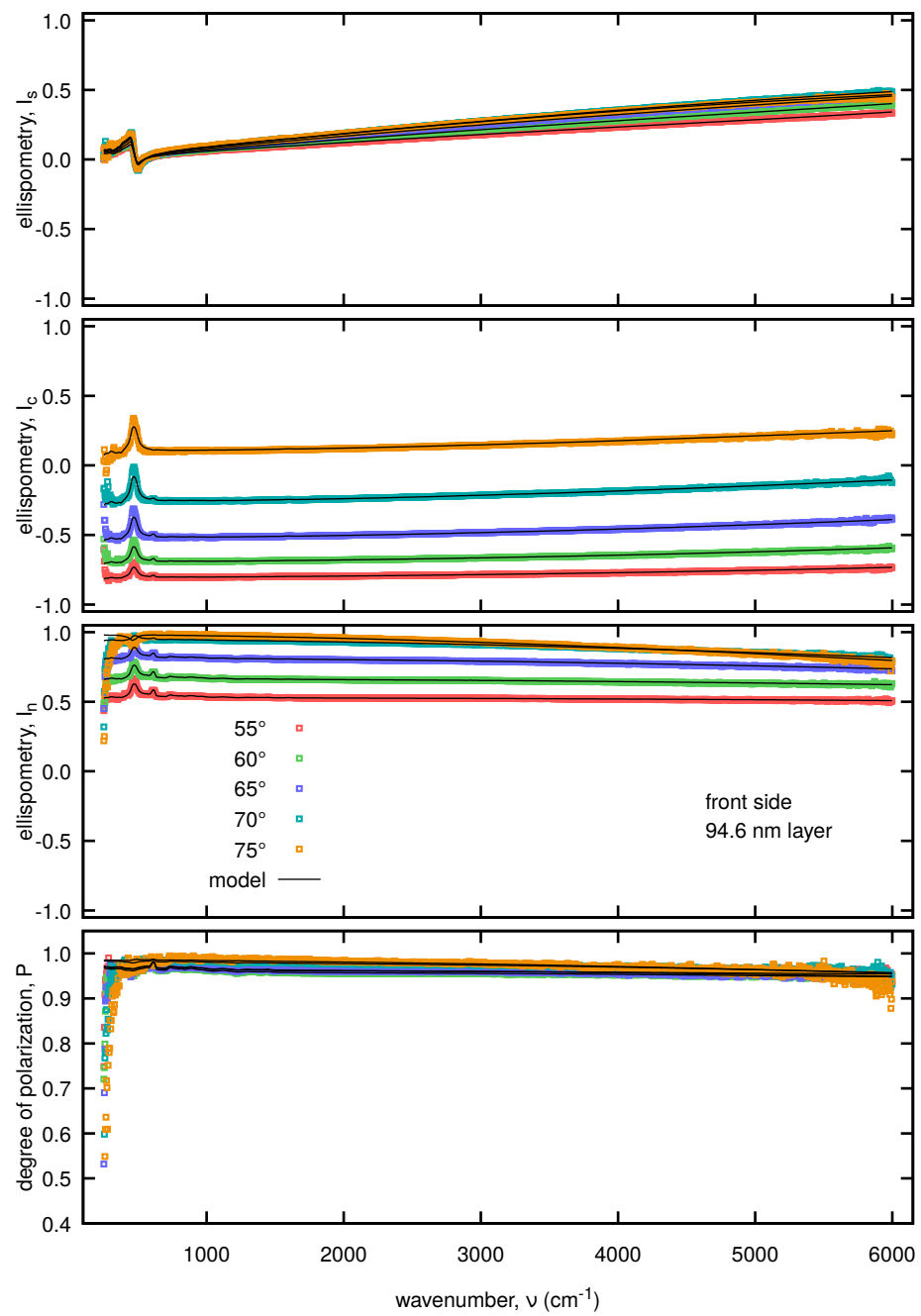


Figure S4. Spectral dependencies of the generalized ellipsometric parameters displayed for the 94.6 nm thick film #4 (measured from the front side).

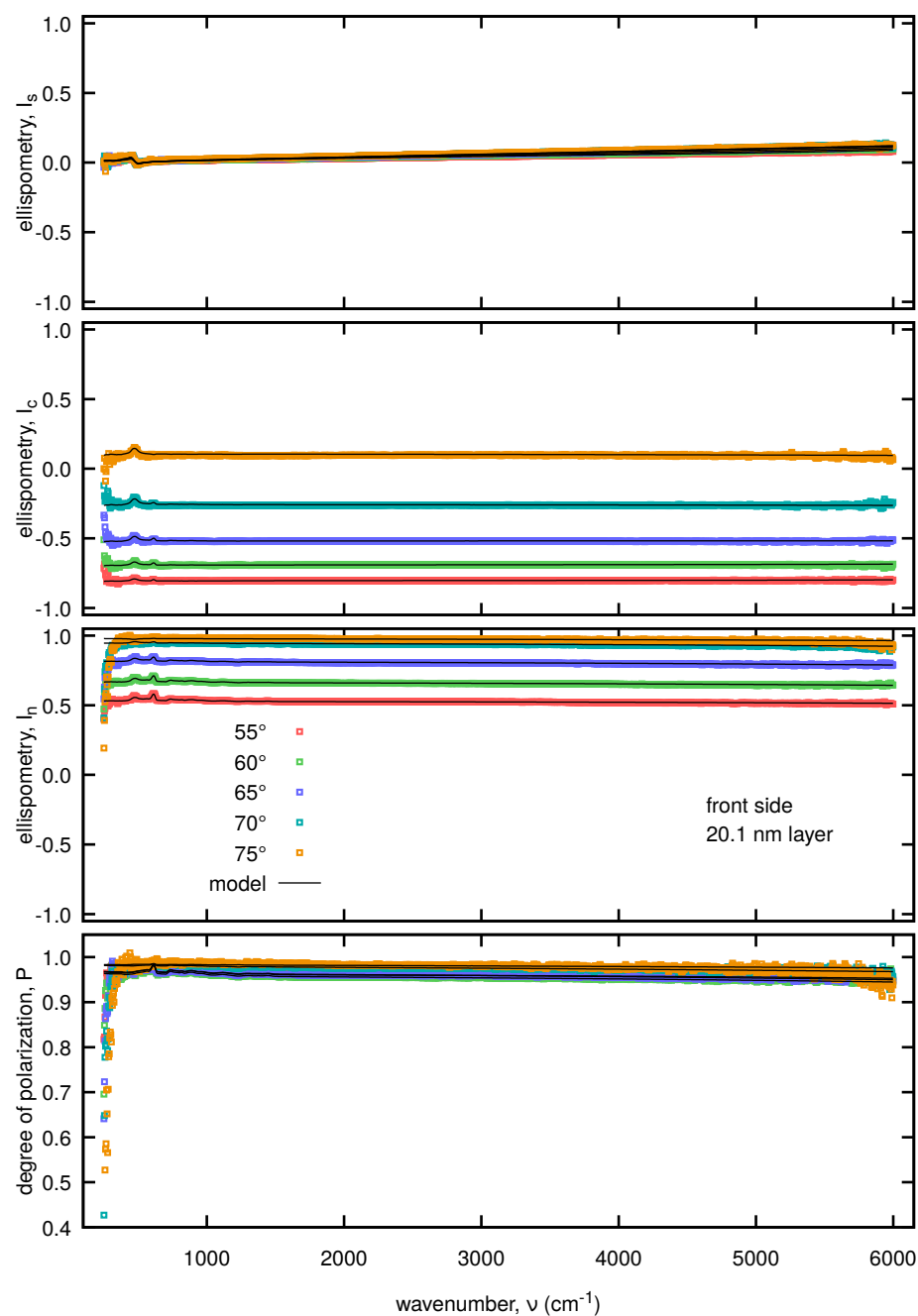


Figure S5. Spectral dependencies of the generalized ellipsometric parameters displayed for the 20.1 nm thick film #5 (measured from the front side).

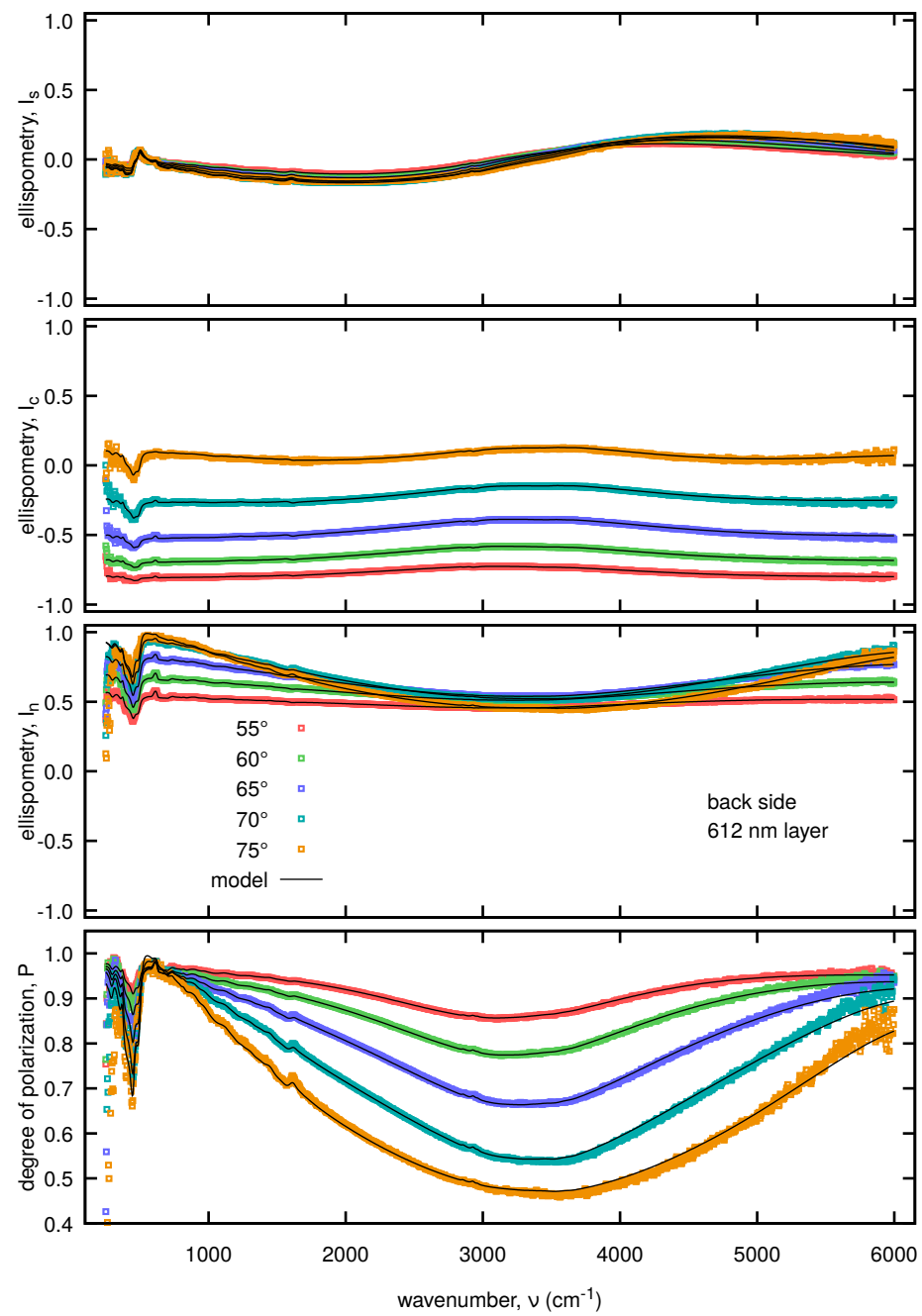


Figure S6. Spectral dependencies of the generalized ellipsometric parameters displayed for the 612 nm thick film #1 (measured from the back side).

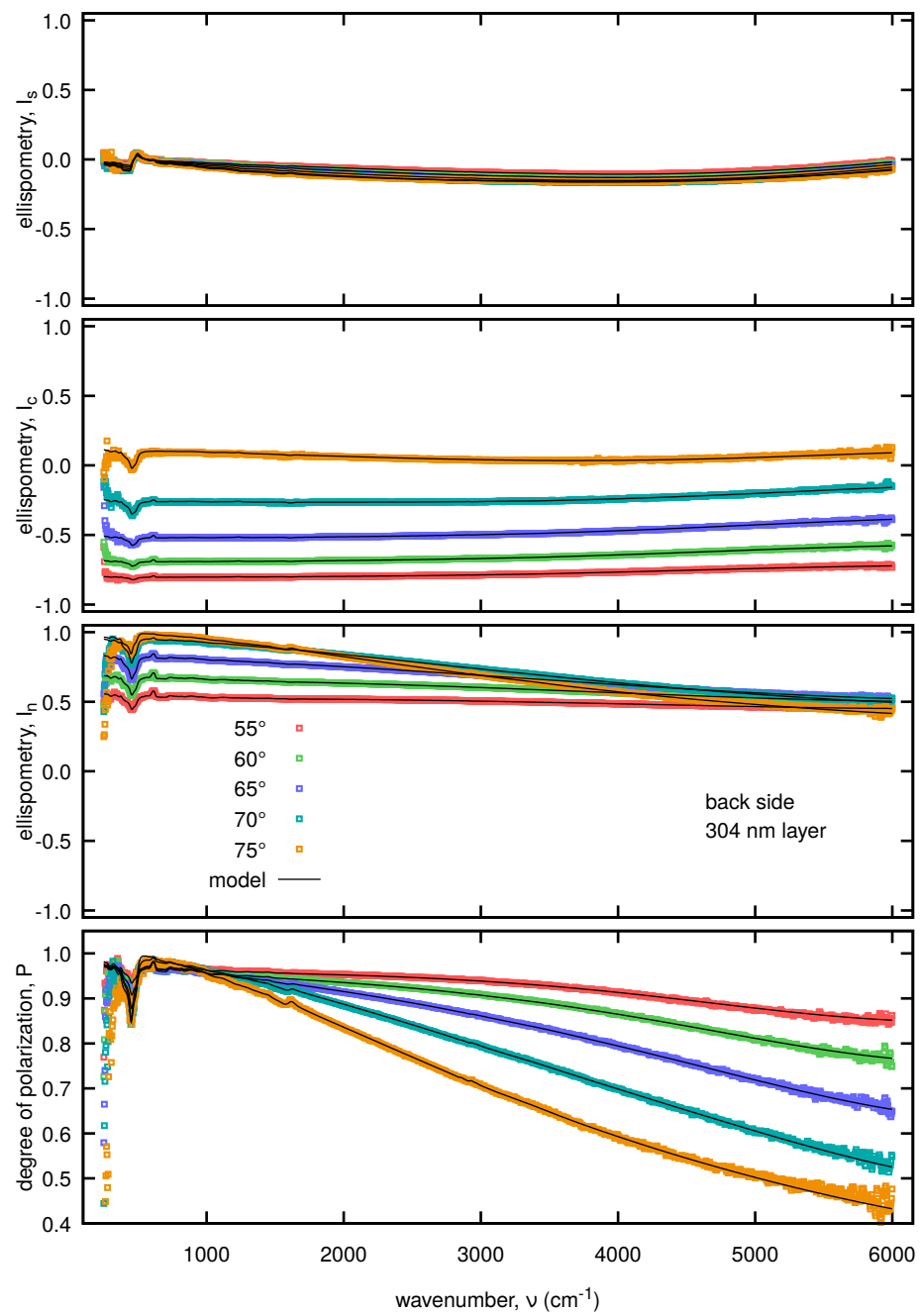


Figure S7. Spectral dependencies of the generalized ellipsometric parameters displayed for the 304 nm thick film #2 (measured from the back side).

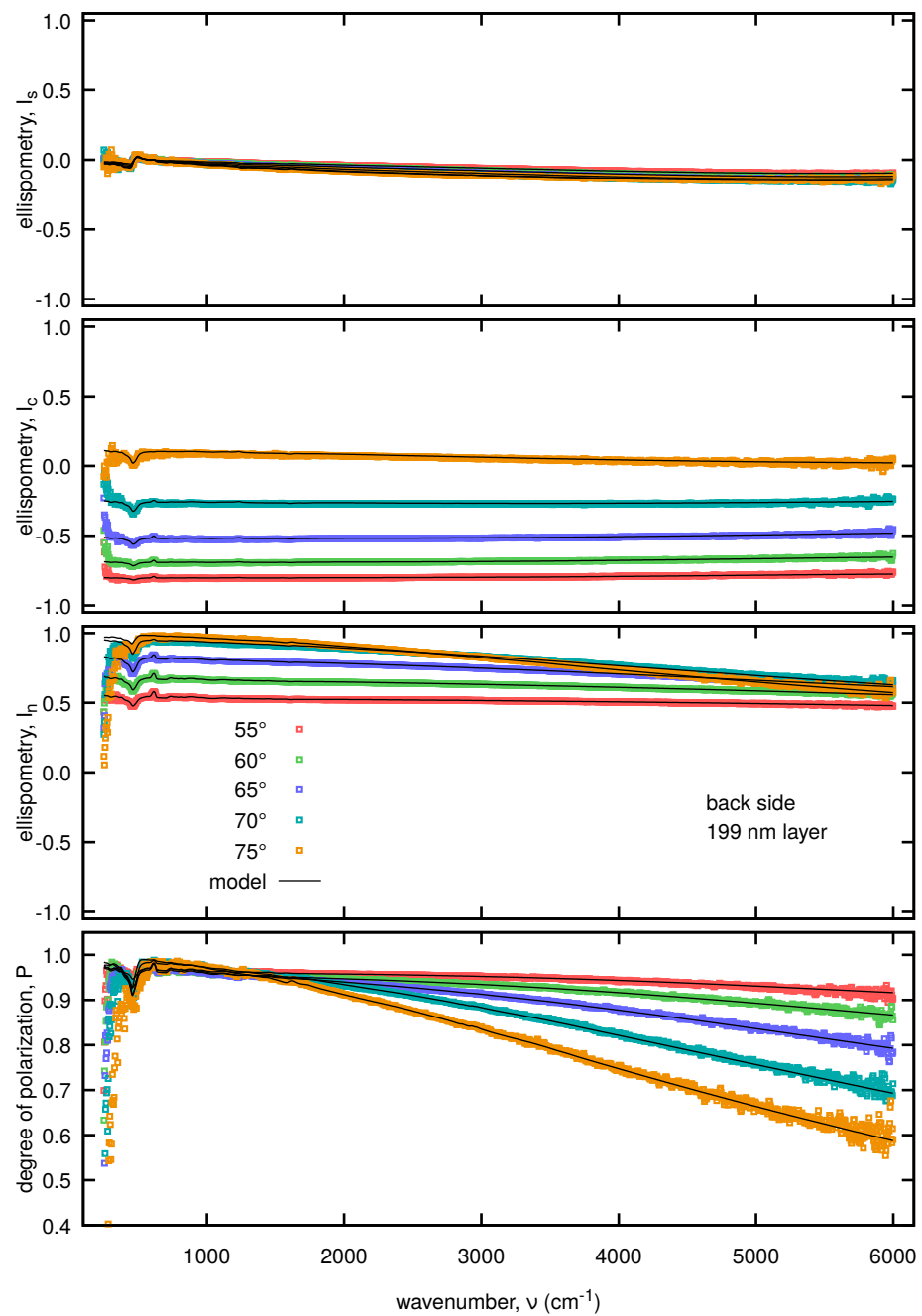


Figure S8. Spectral dependencies of the generalized ellipsometric parameters displayed for the 199 nm thick film #3 (measured from the back side).

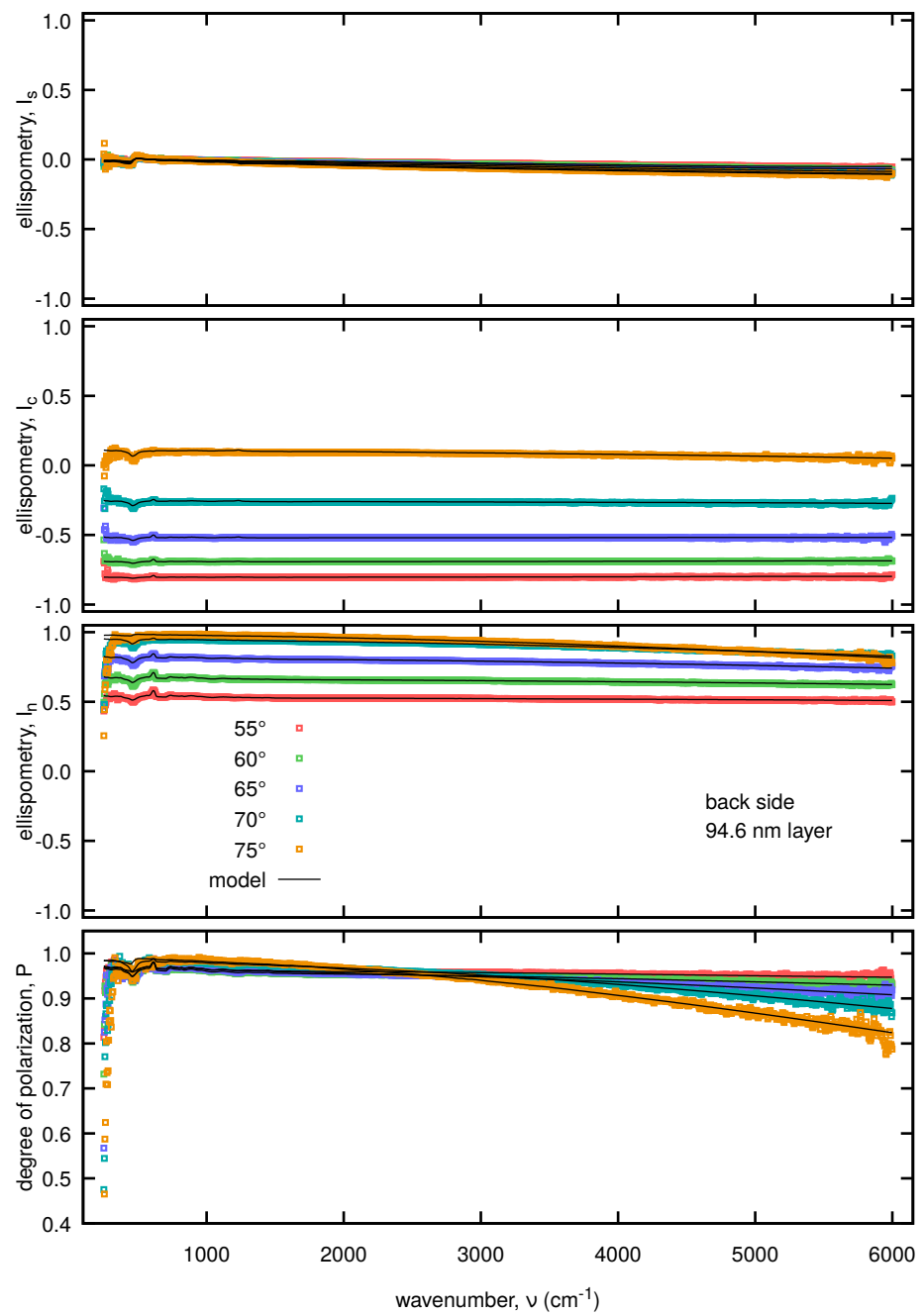


Figure S9. Spectral dependencies of the generalized ellipsometric parameters displayed for the 94.6 nm thick film #4 (measured from the back side).

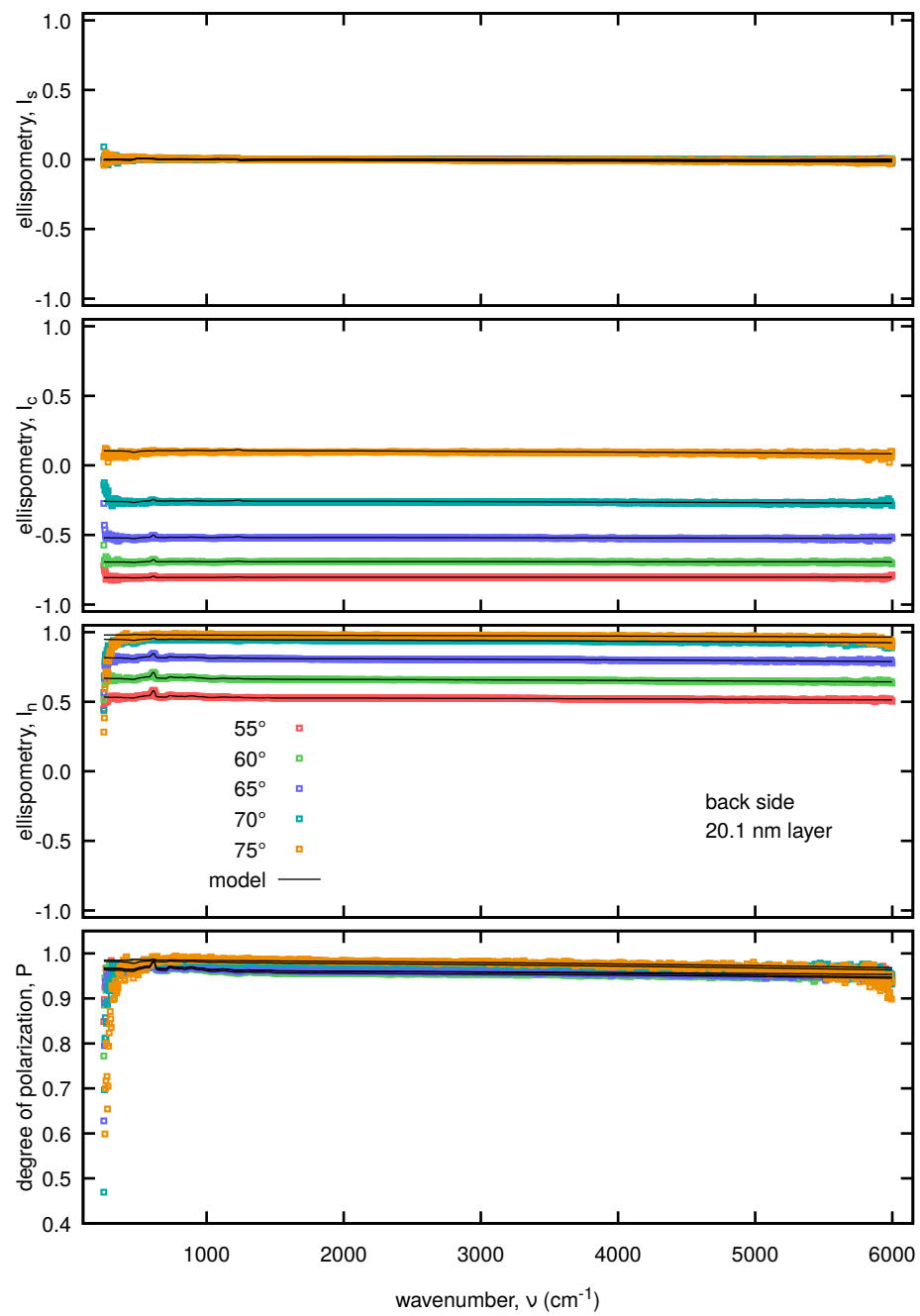


Figure S10. Spectral dependencies of the generalized ellipsometric parameters displayed for the 20.1 nm thick film #5 (measured from the back side).

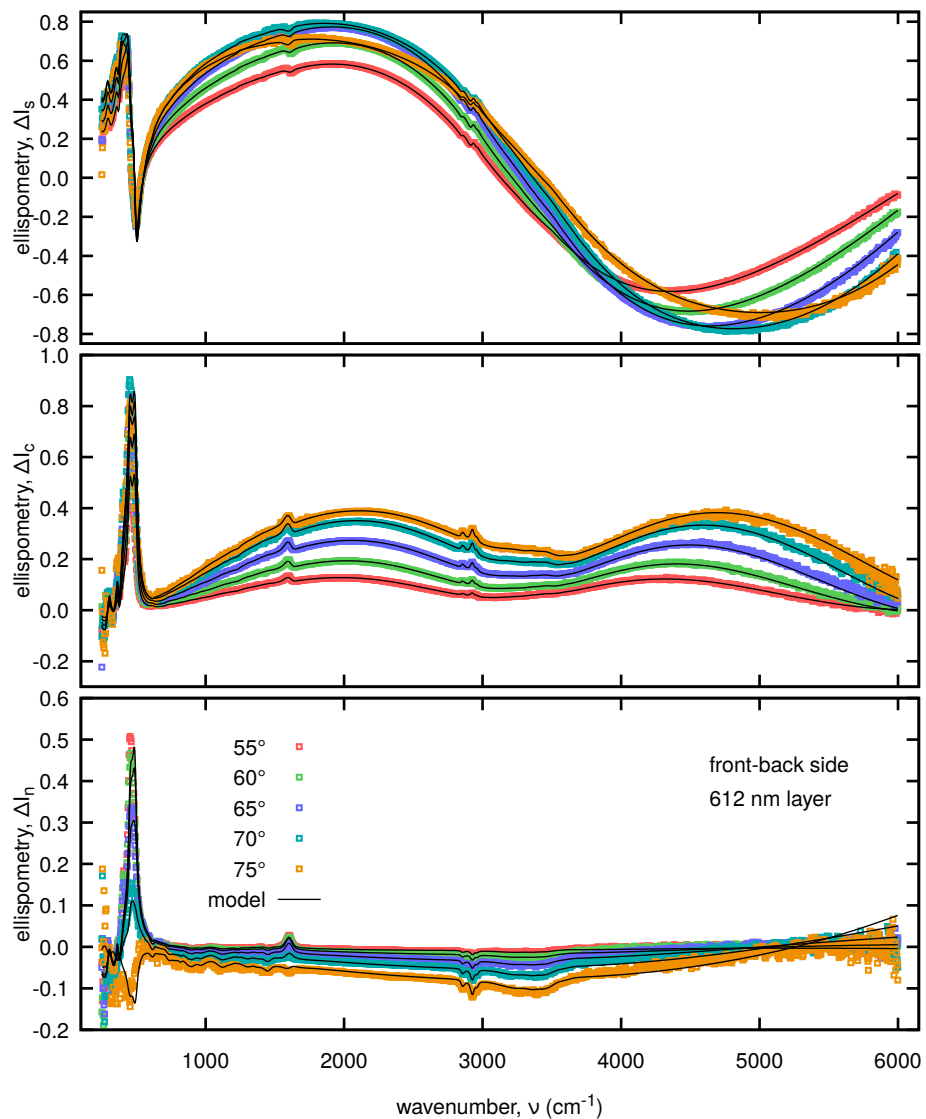


Figure S11. Spectral dependencies of the difference ellipsometric quantities displayed for the 612 nm thick film #1.

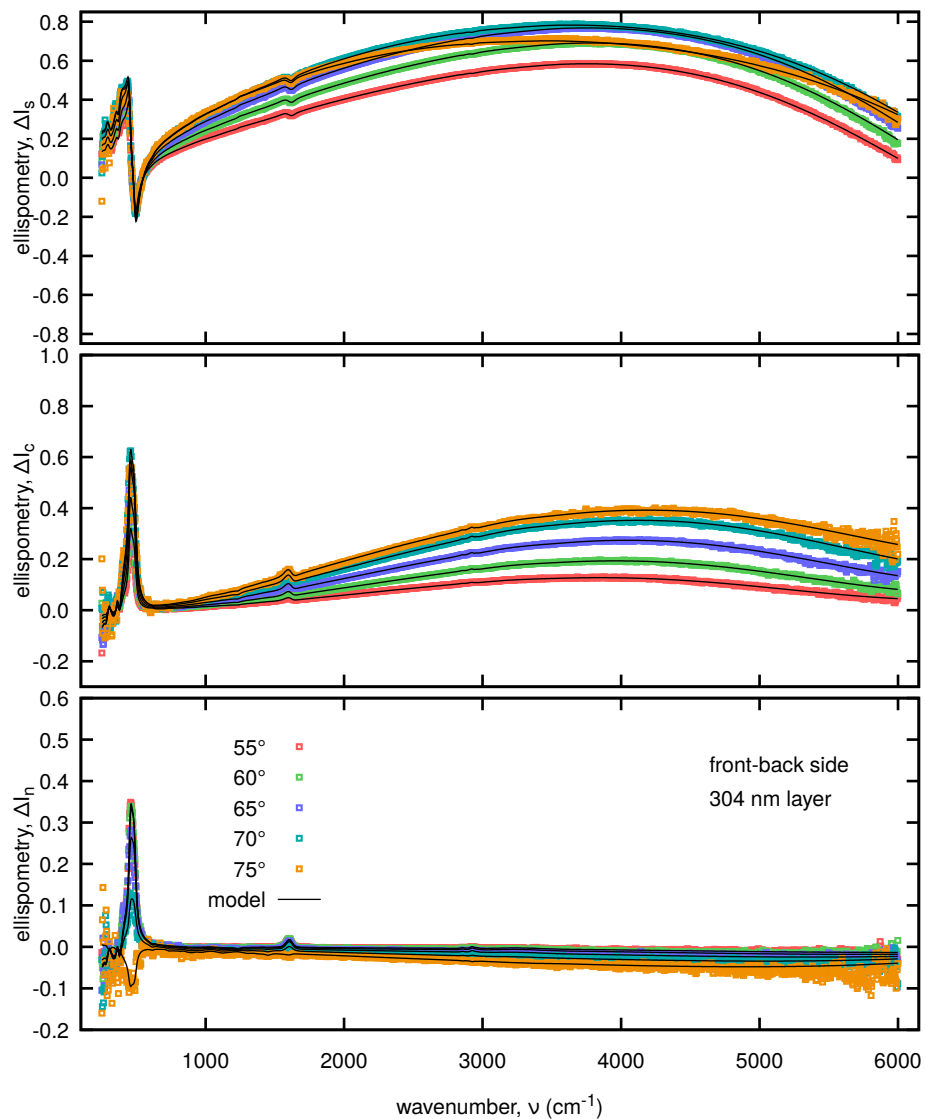


Figure S12. Spectral dependencies of the difference ellipsometric quantities displayed for the 304 nm thick film #2.

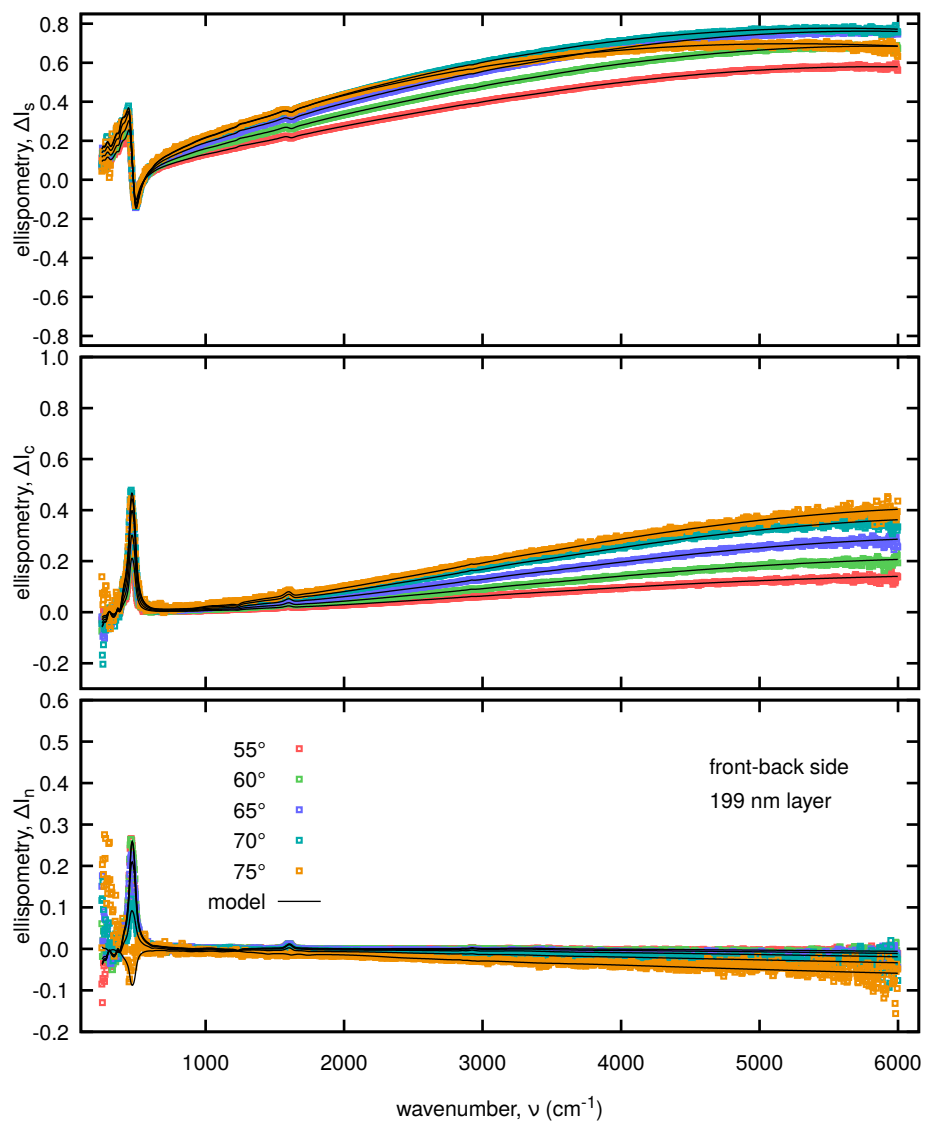


Figure S13. Spectral dependencies of the difference ellipsometric quantities displayed for the 199 nm thick film #3.

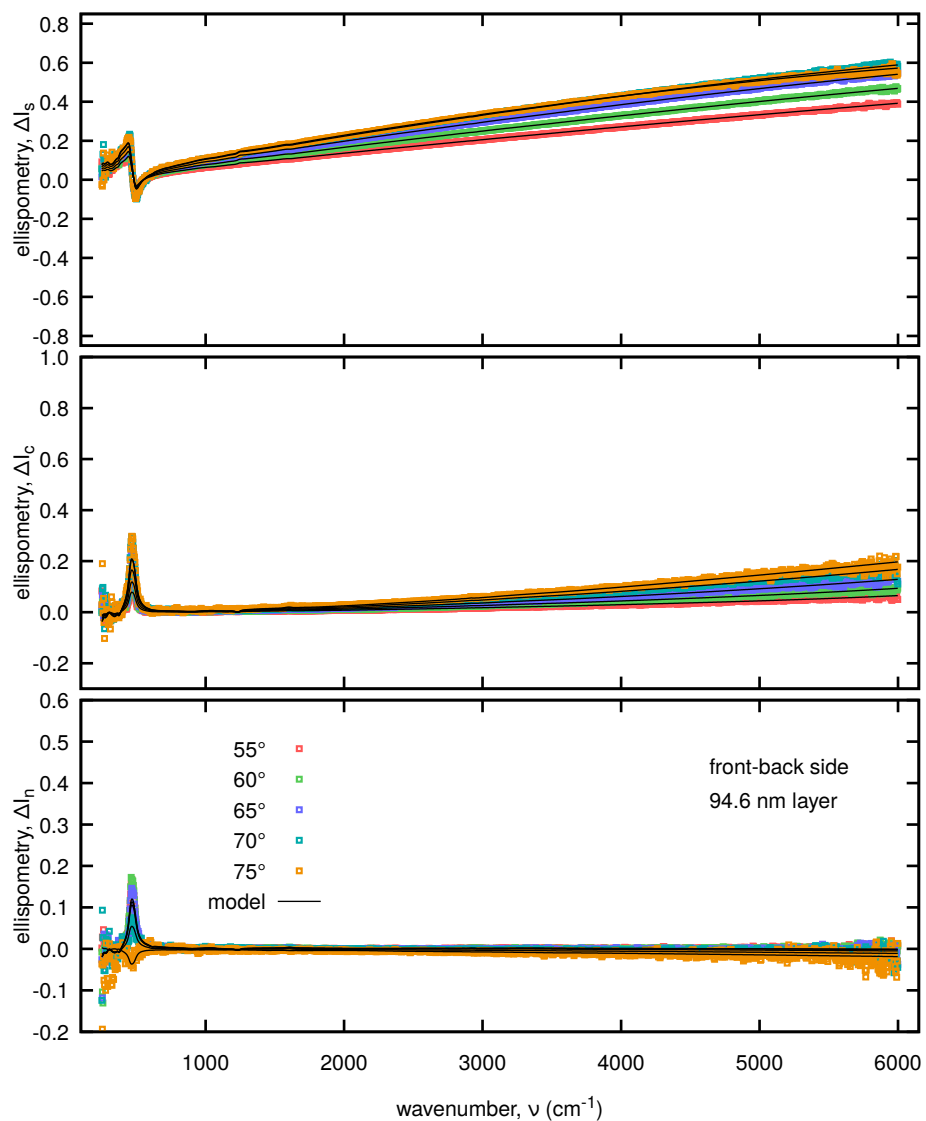


Figure S14. Spectral dependencies of the difference ellipsometric quantities displayed for the 94.6 nm thick film #4.

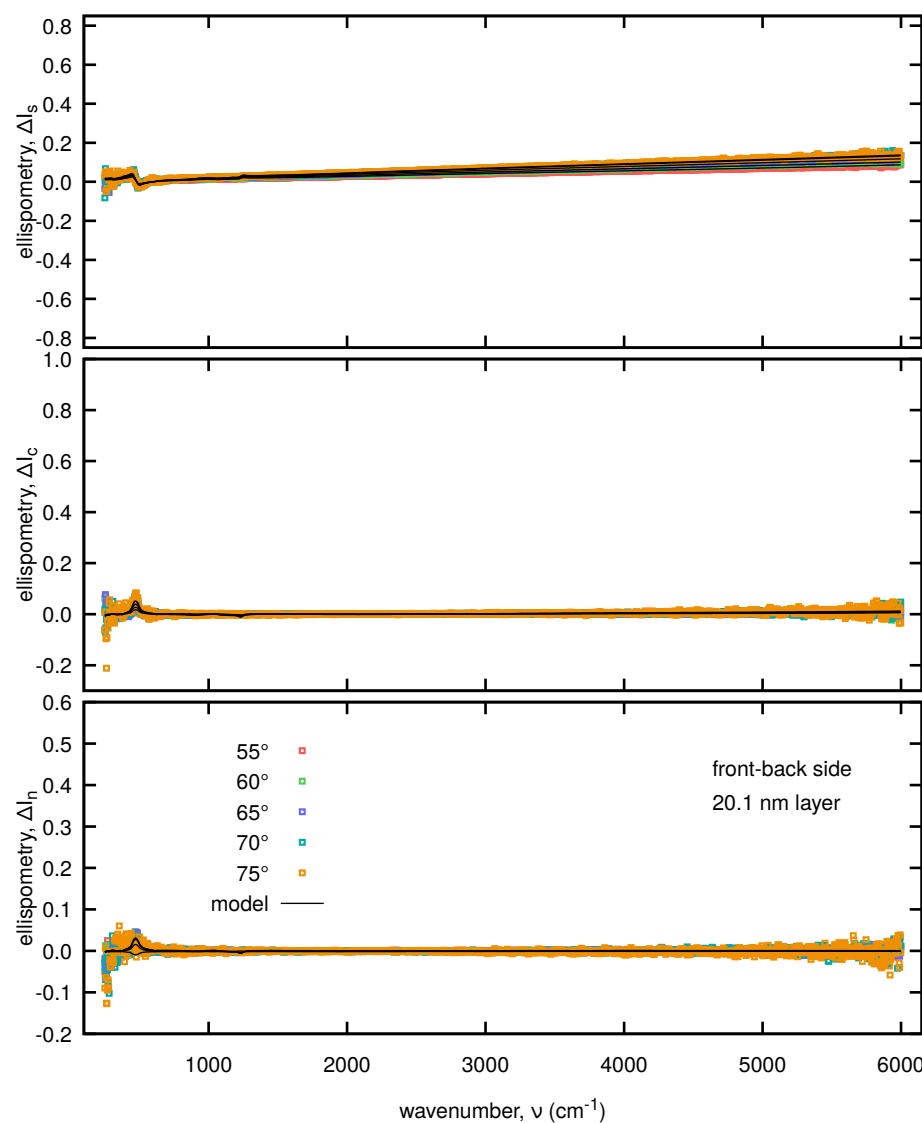


Figure S15. Spectral dependencies of the difference ellipsometric quantities displayed for the 20.1 nm thick film #5.

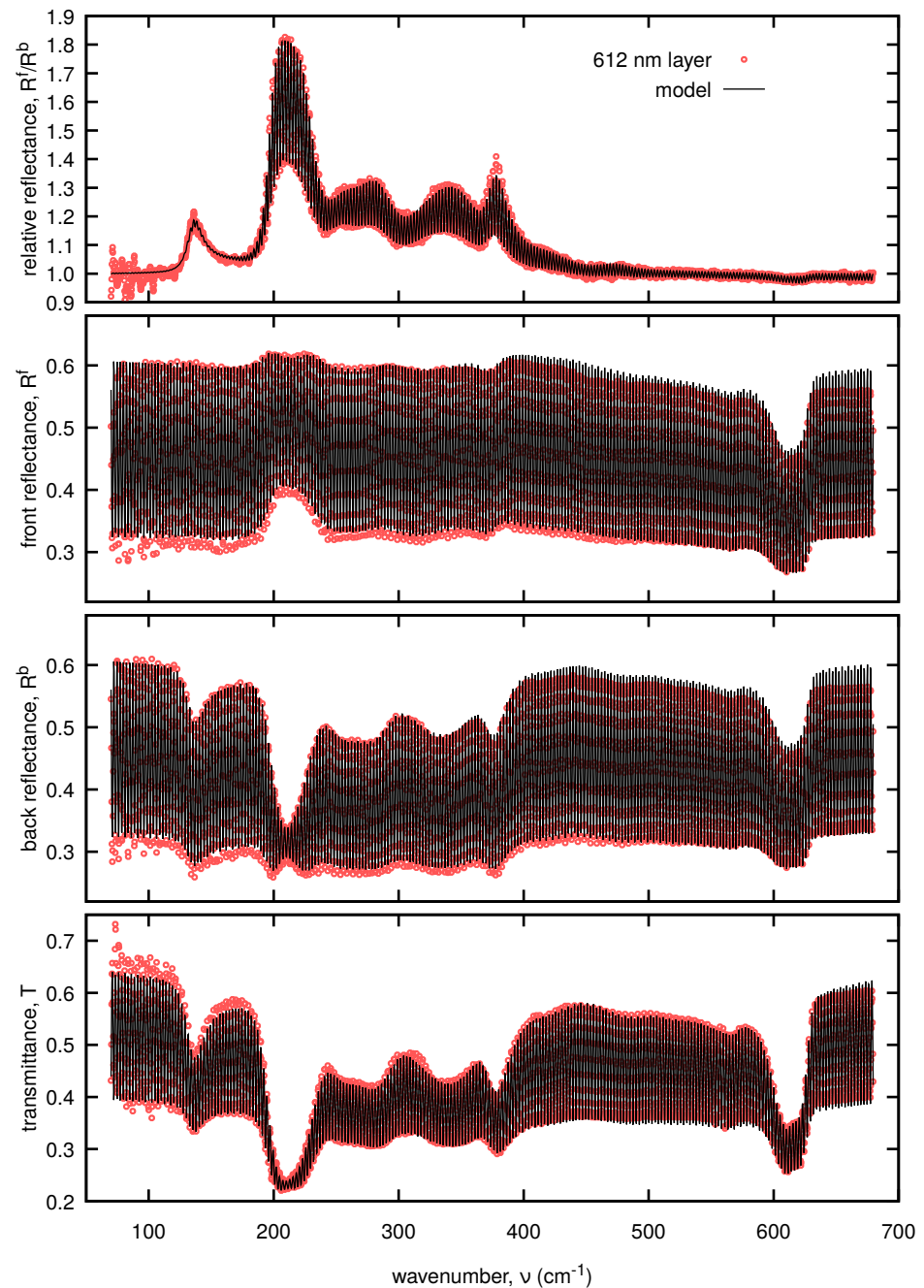


Figure S16. Spectral dependencies of the spectrophotometric quantities displayed for the 612 nm thick film.

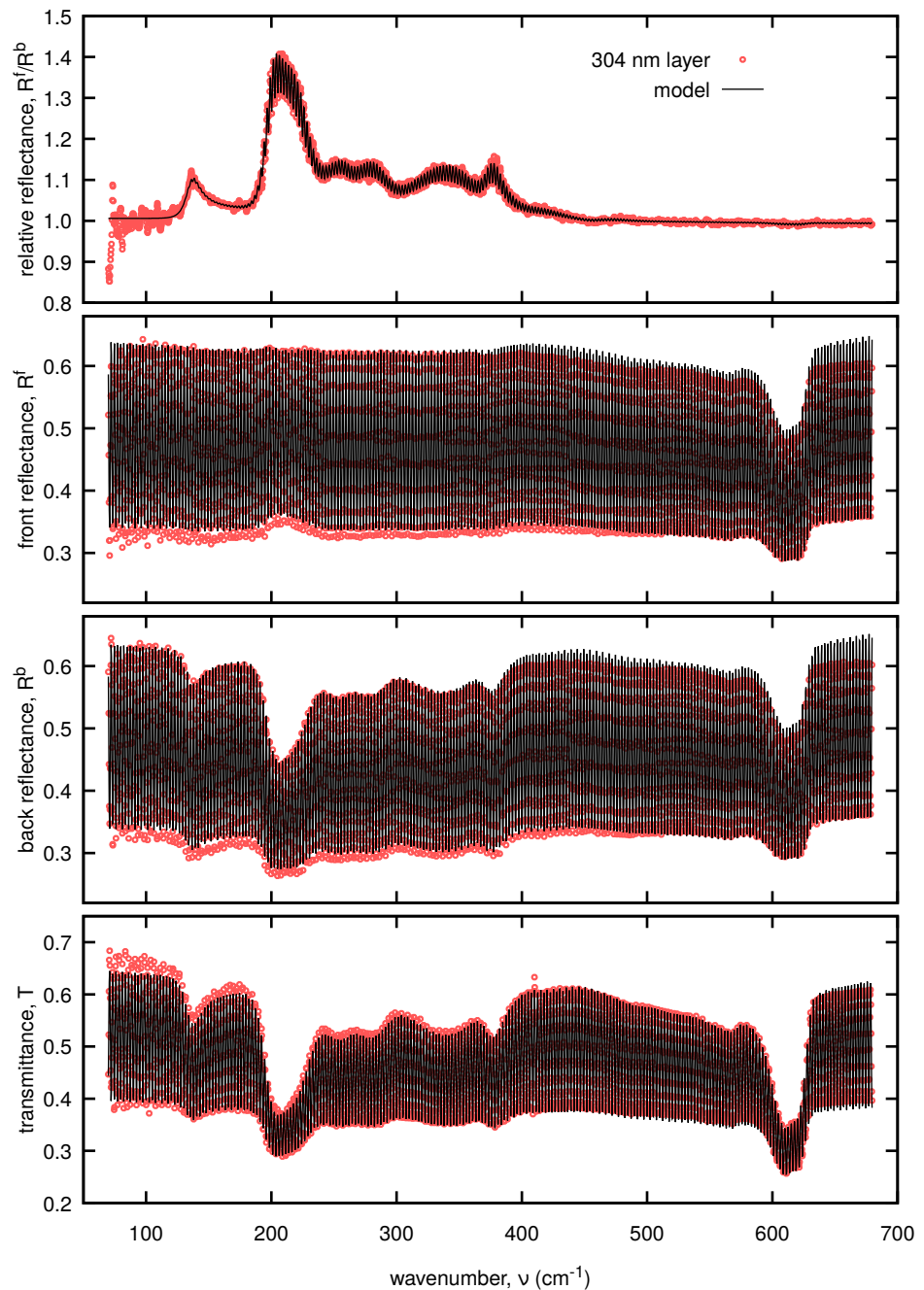


Figure S17. Spectral dependencies of the spectrophotometric quantities displayed for the 304 nm thick film.

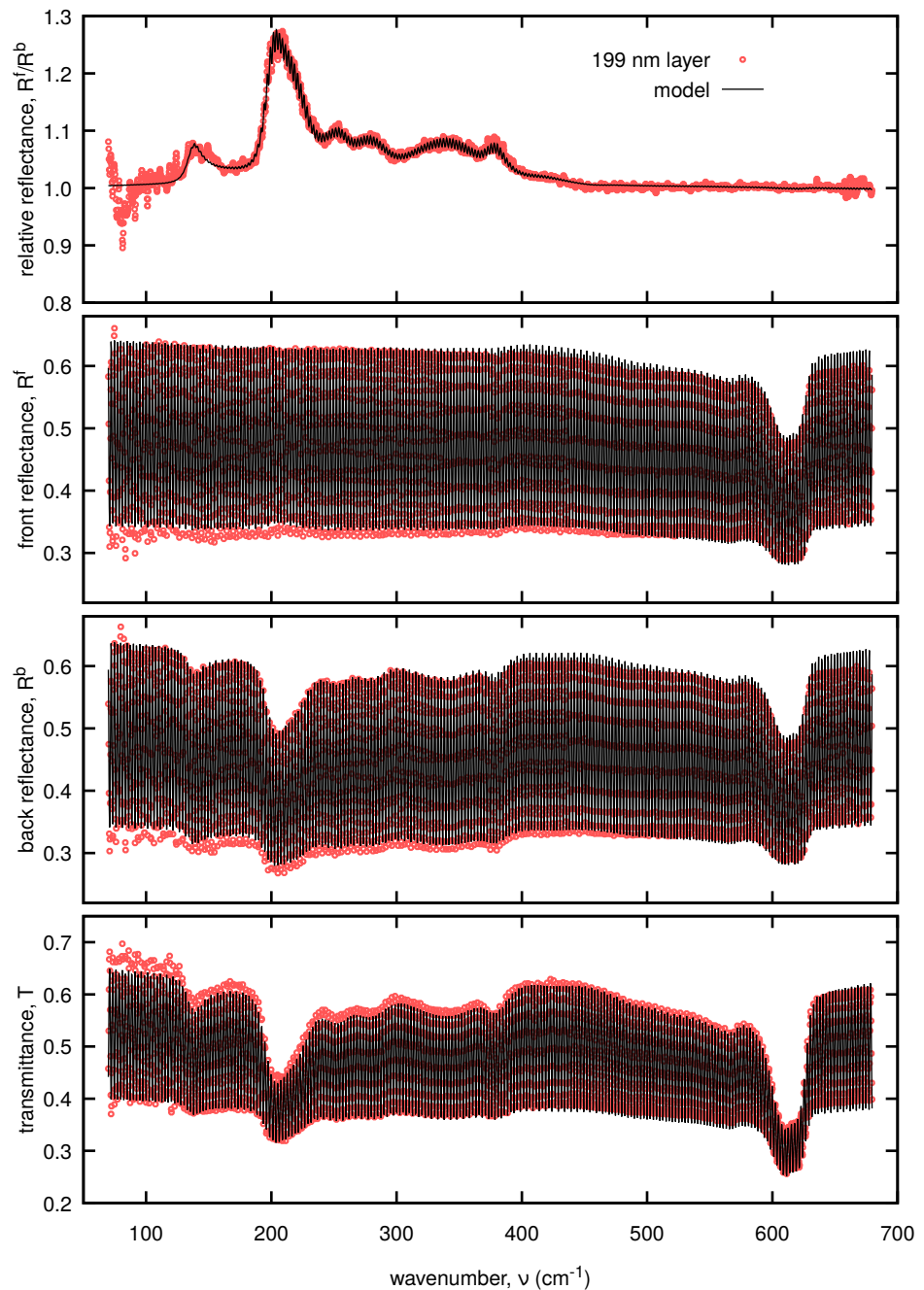


Figure S18. Spectral dependencies of the spectrophotometric quantities displayed for the 199 nm thick film.

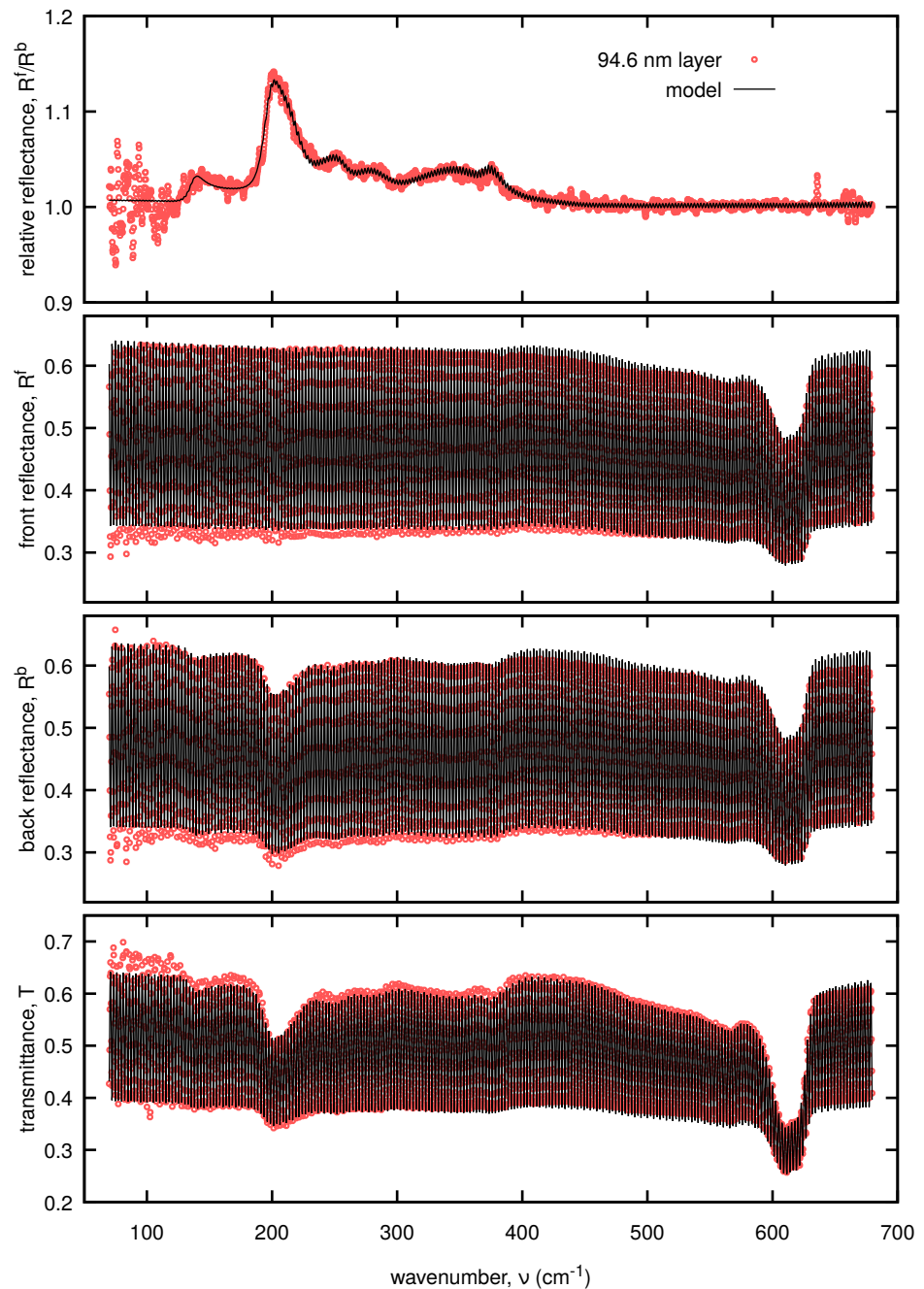


Figure S19. Spectral dependencies of the spectrophotometric quantities displayed for the 94.6 nm thick film.

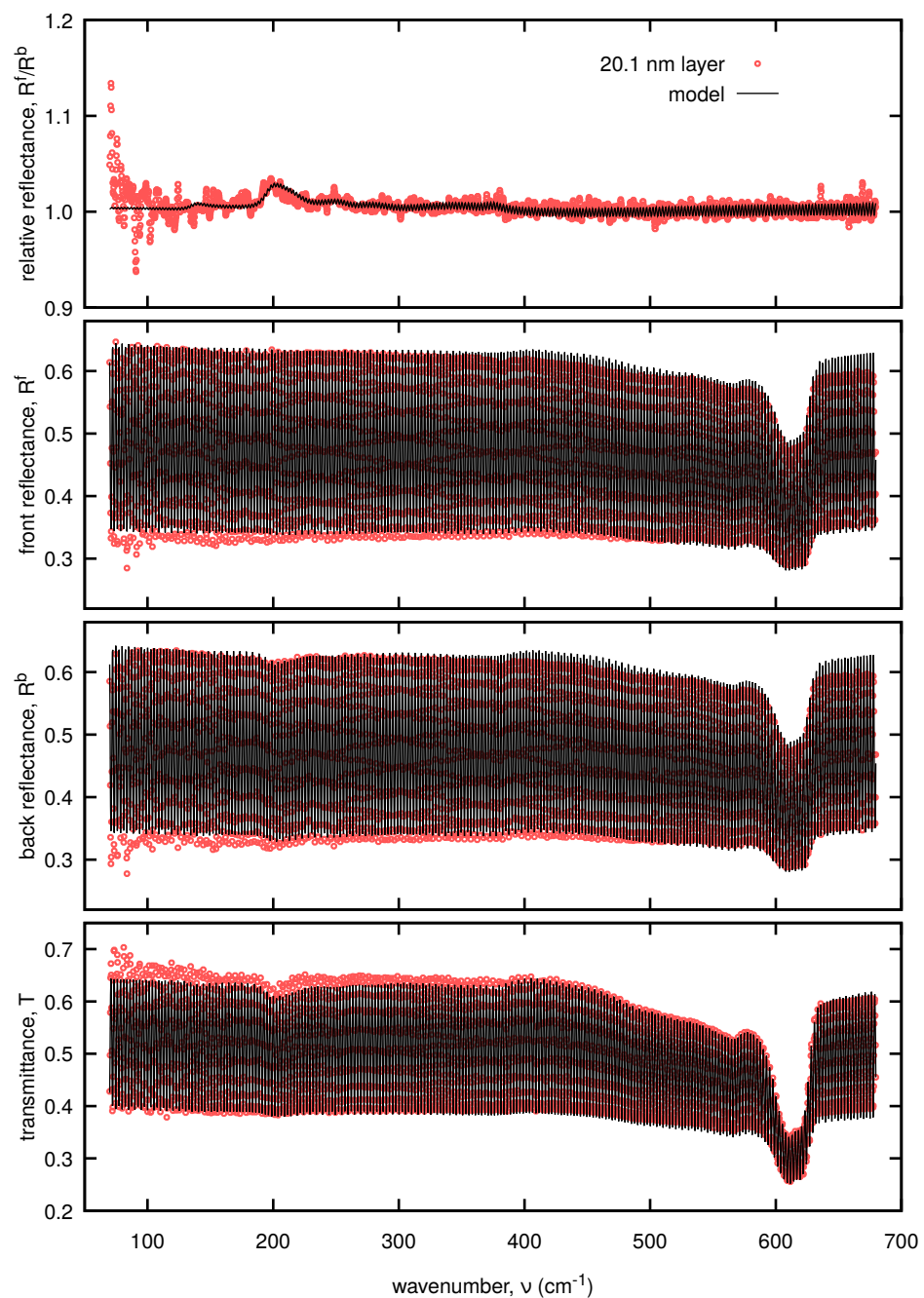


Figure S20. Spectral dependencies of the spectrophotometric quantities displayed for the 20.1 nm thick film.

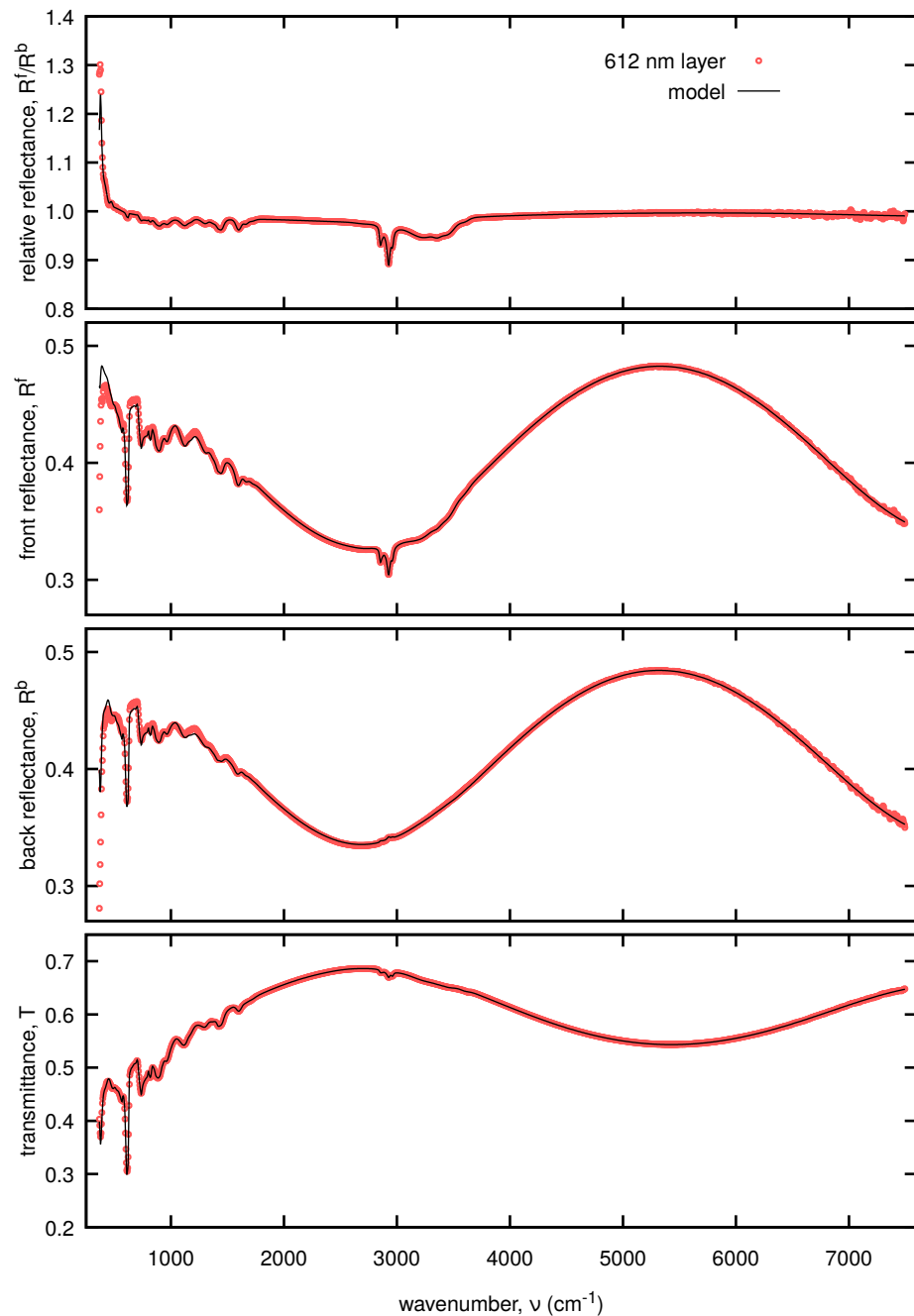


Figure S21. Spectral dependencies of the spectrophotometric quantities displayed for the 612 nm thick film.

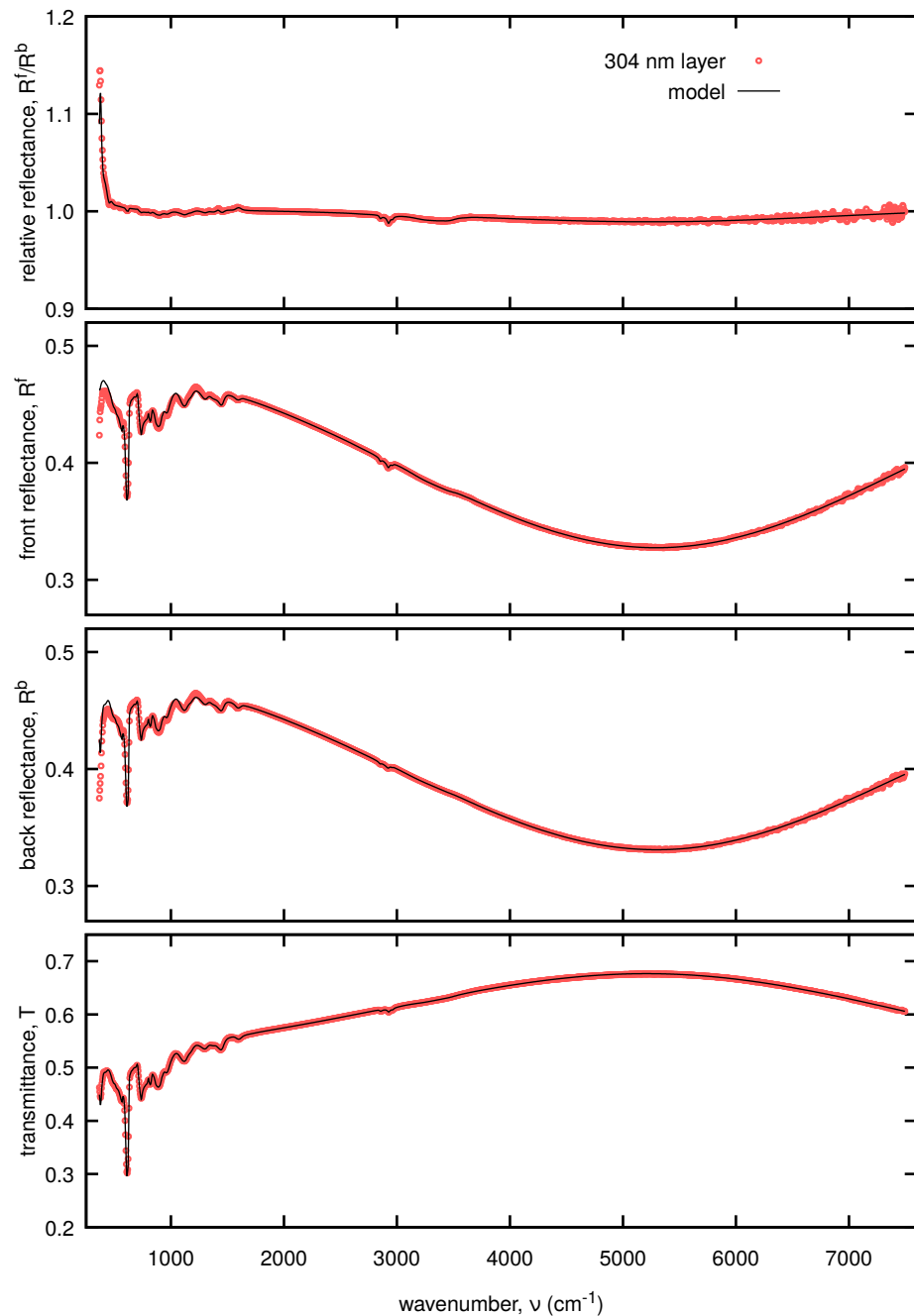


Figure S22. Spectral dependencies of the spectrophotometric quantities displayed for the 304 nm thick film.

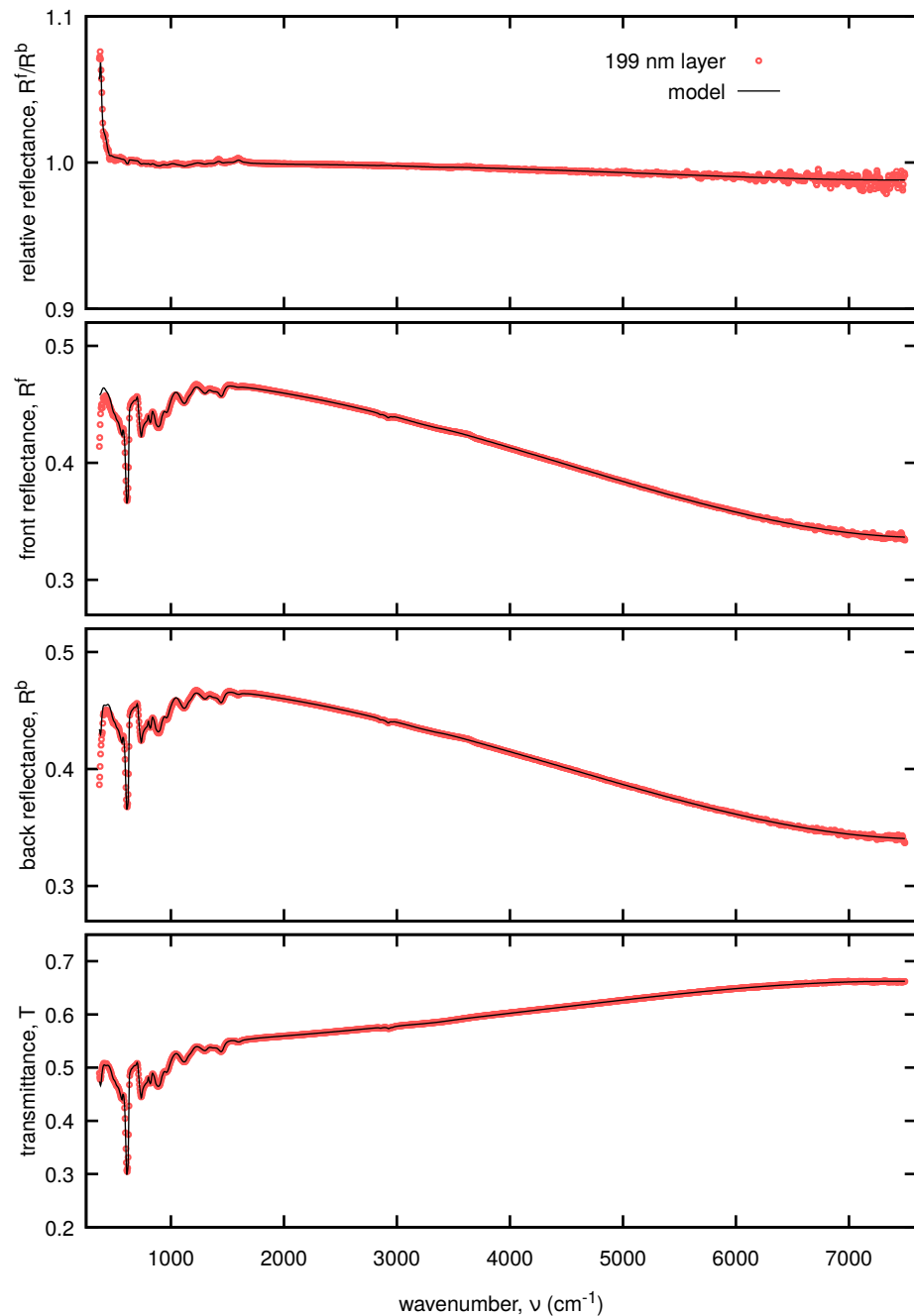


Figure S23. Spectral dependencies of the spectrophotometric quantities displayed for the 199 nm thick film.

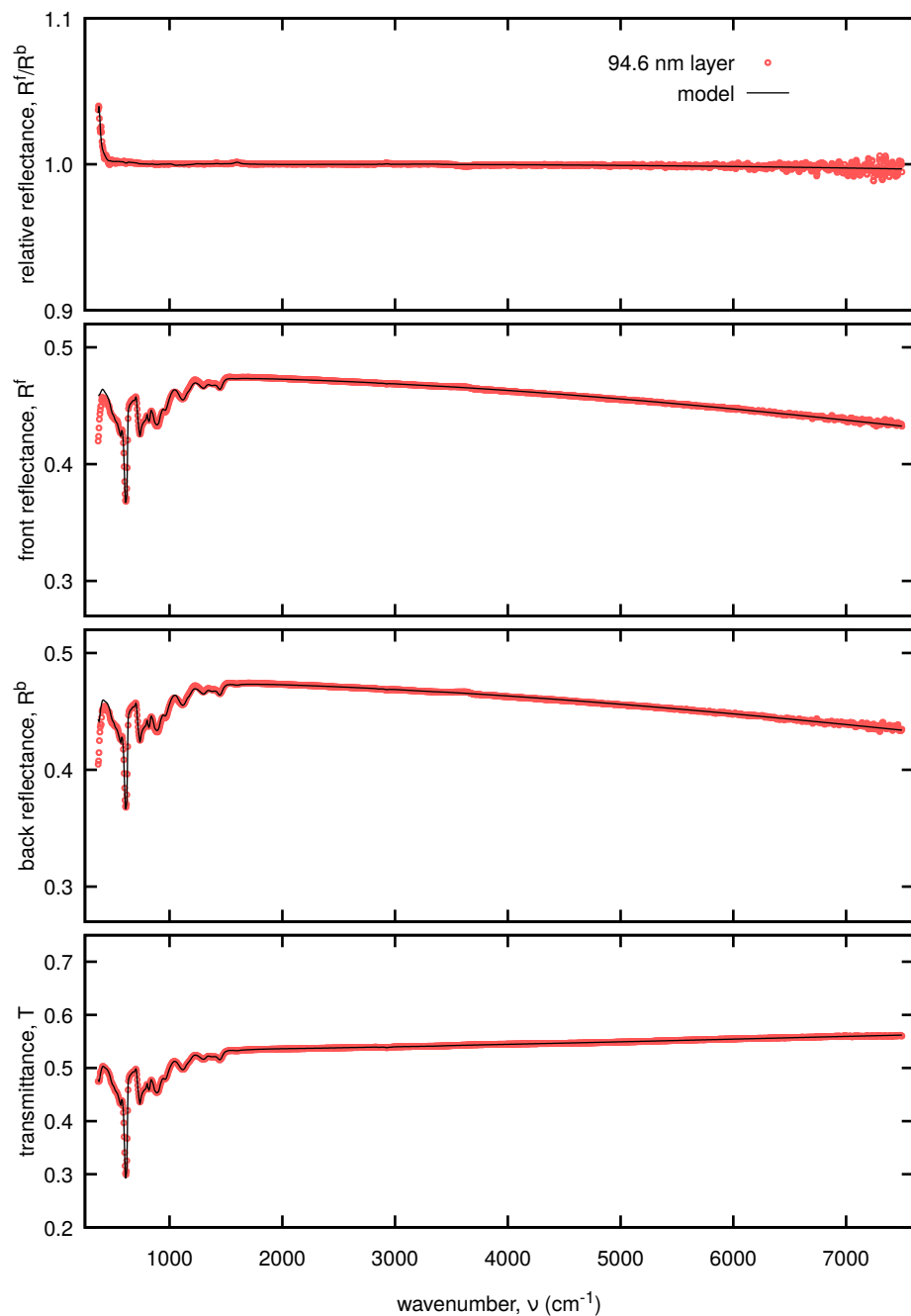


Figure S24. Spectral dependencies of the spectrophotometric quantities displayed for the 94.6 nm thick film.

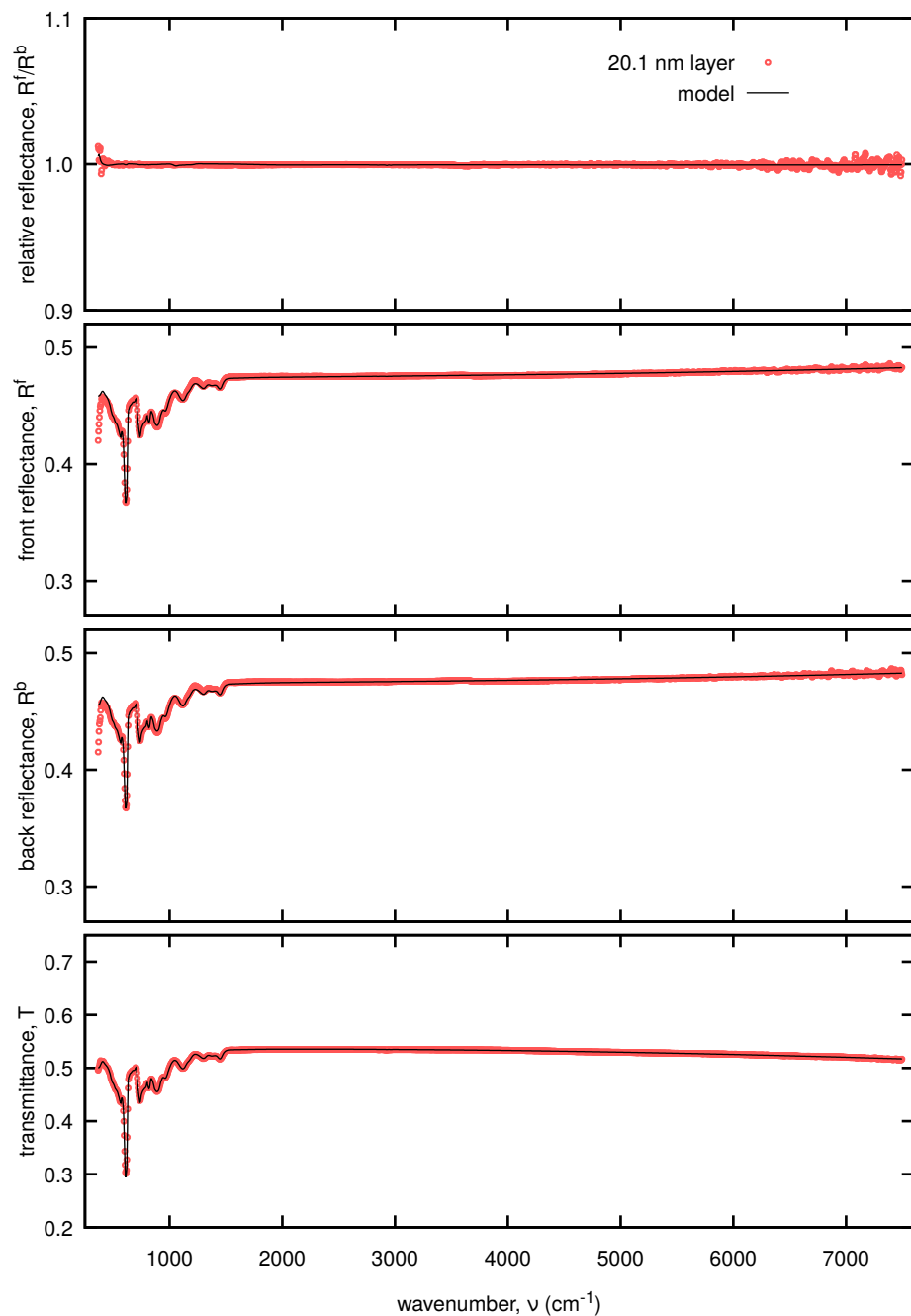


Figure S25. Spectral dependencies of the spectrophotometric quantities displayed for the 20.1 nm thick film.

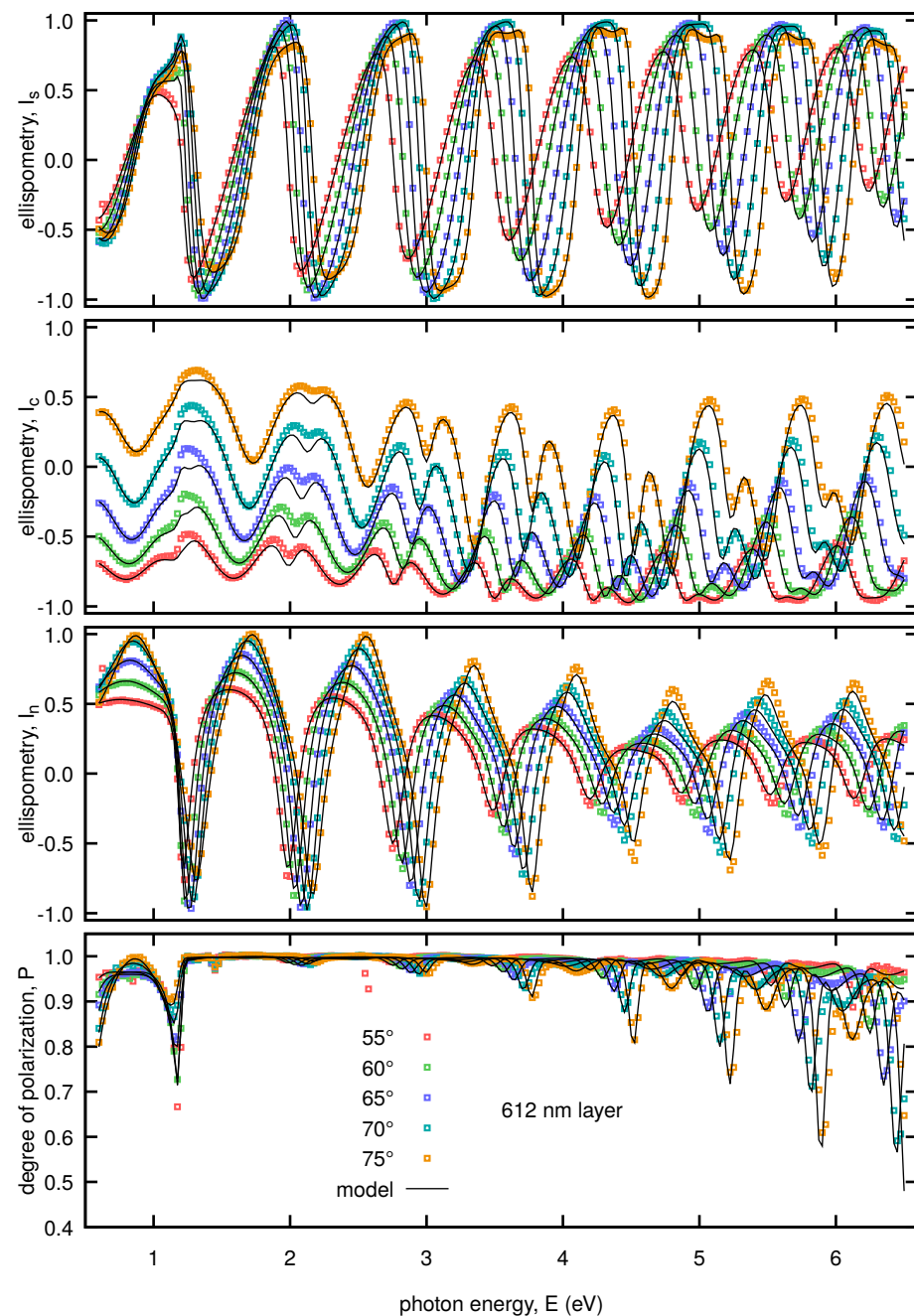


Figure S26. Spectral dependencies of the generalized ellipsometric parameters displayed for the 612 nm thick film (first measurement).

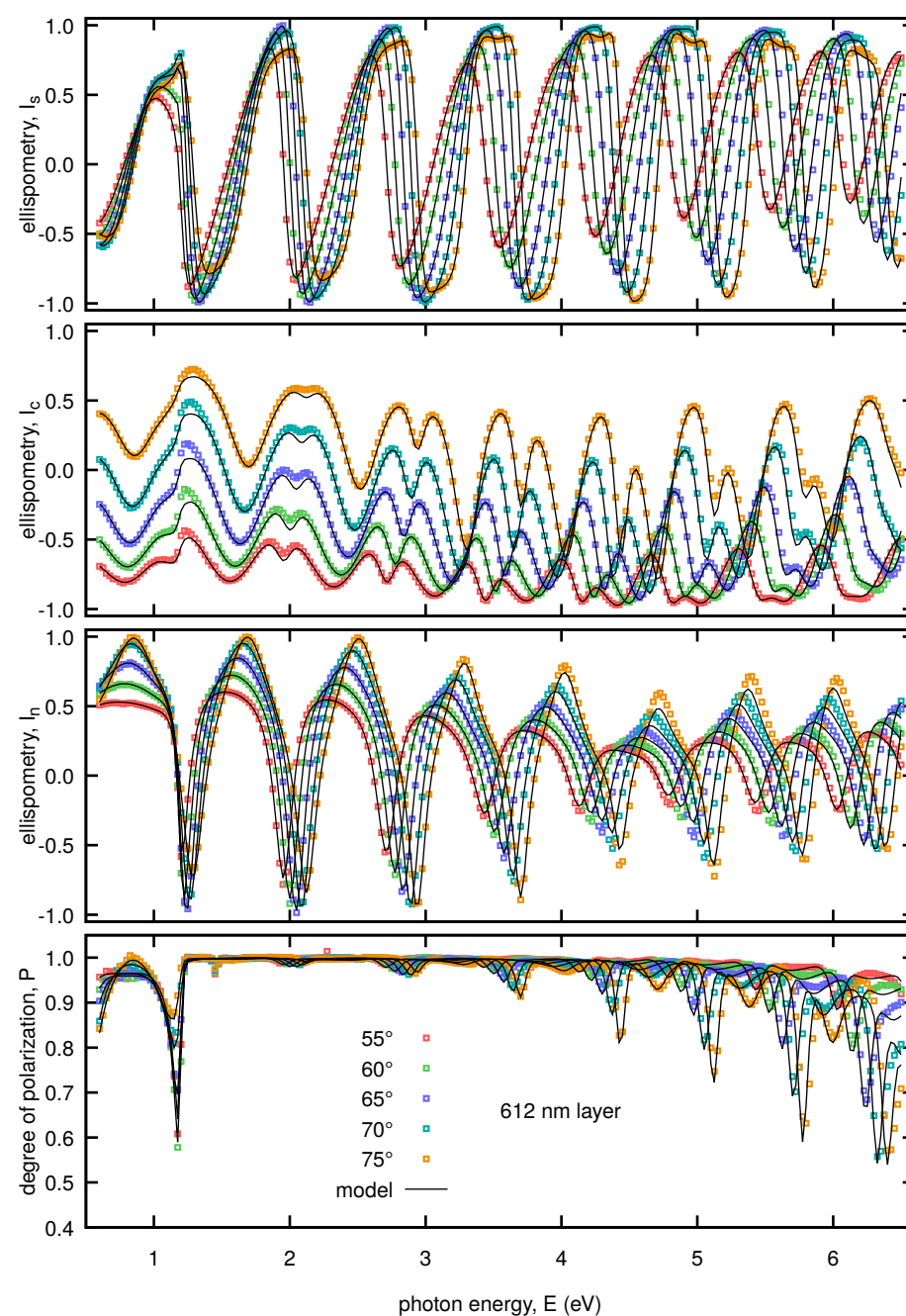


Figure S27. Spectral dependencies of the generalized ellipsometric parameters displayed for the 612 nm thick film (second measurement).

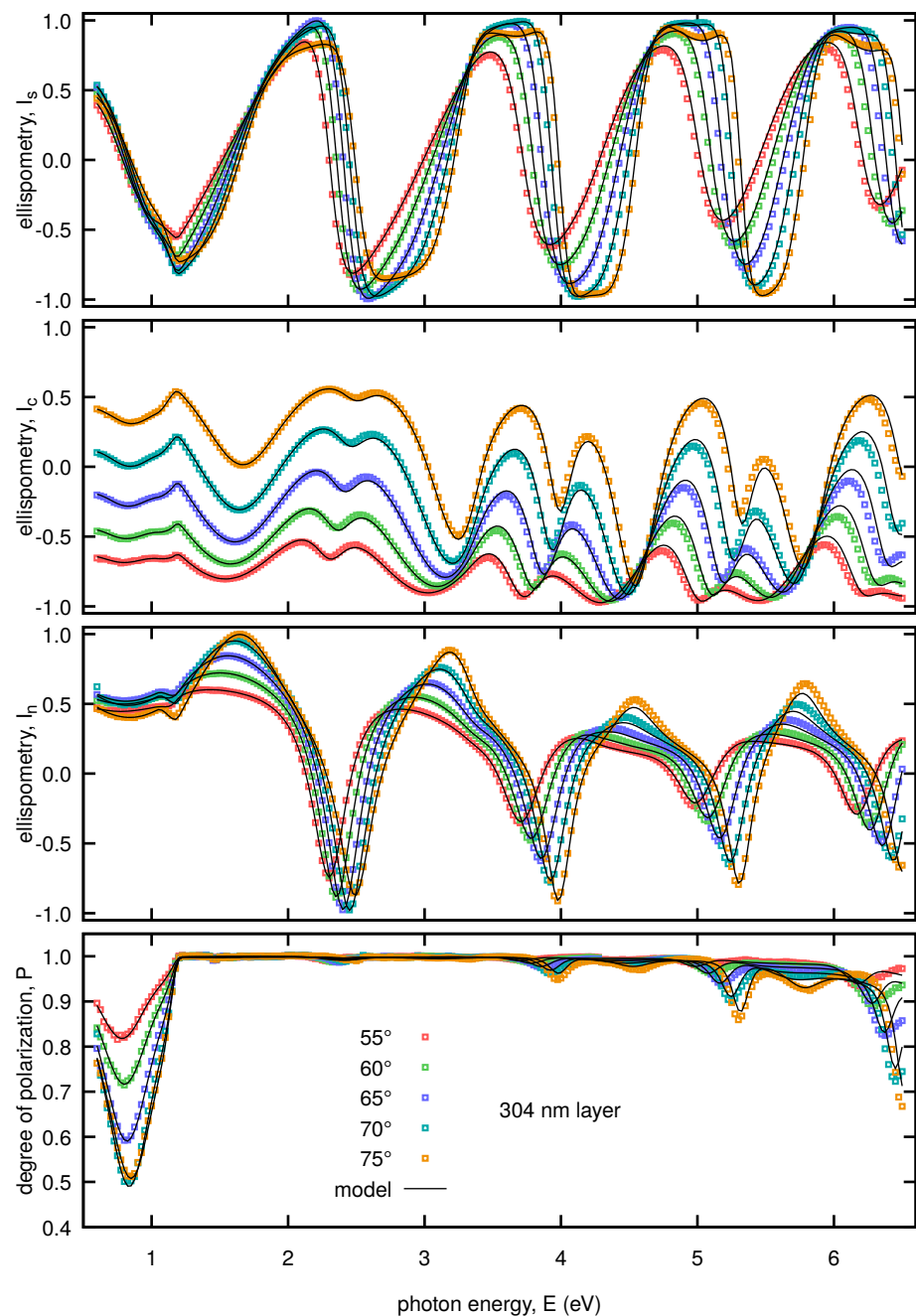


Figure S28. Spectral dependencies of the generalized ellipsometric parameters displayed for the 304 nm thick film.

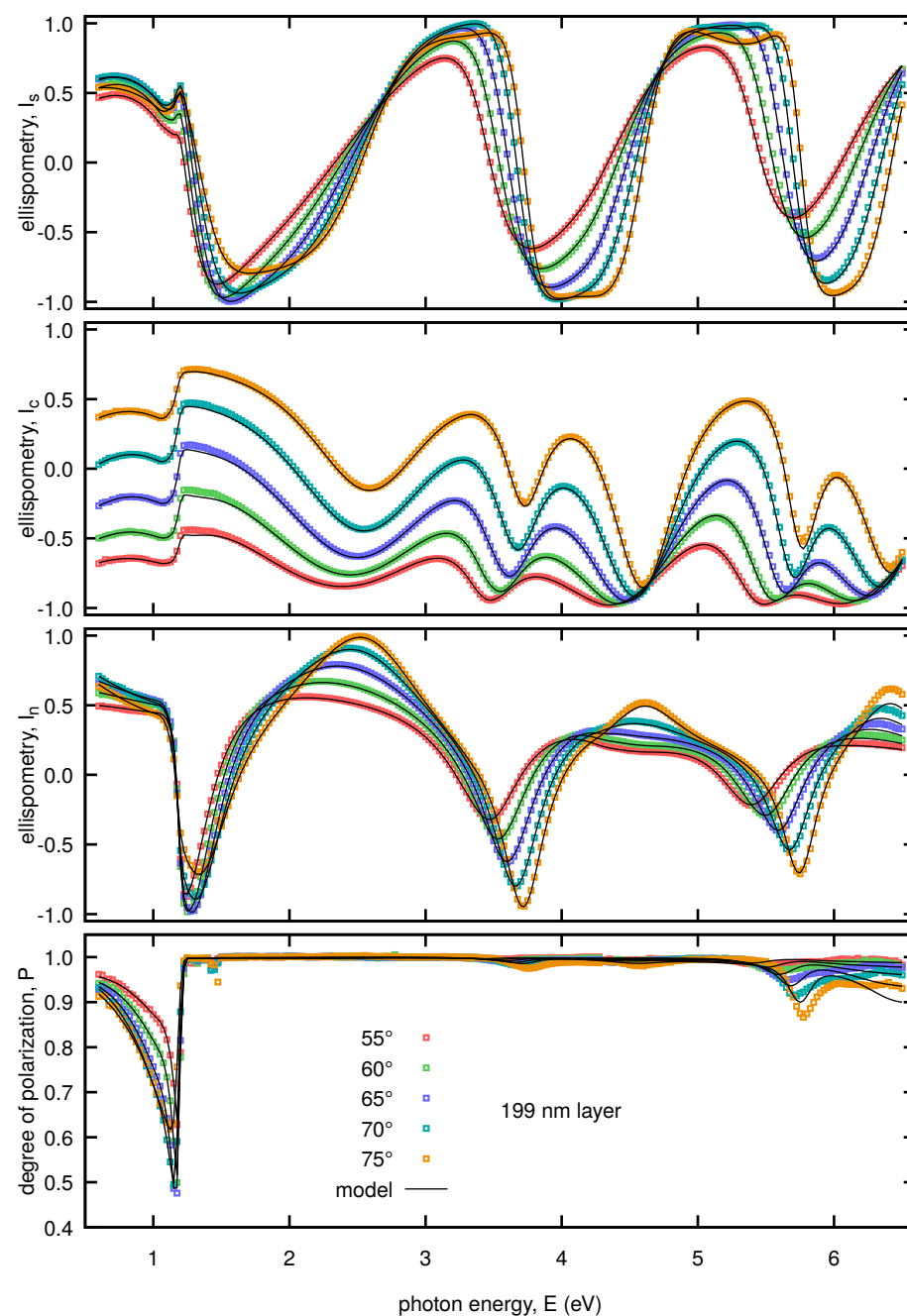


Figure S29. Spectral dependencies of the generalized ellipsometric parameters displayed for the 199 nm thick film.

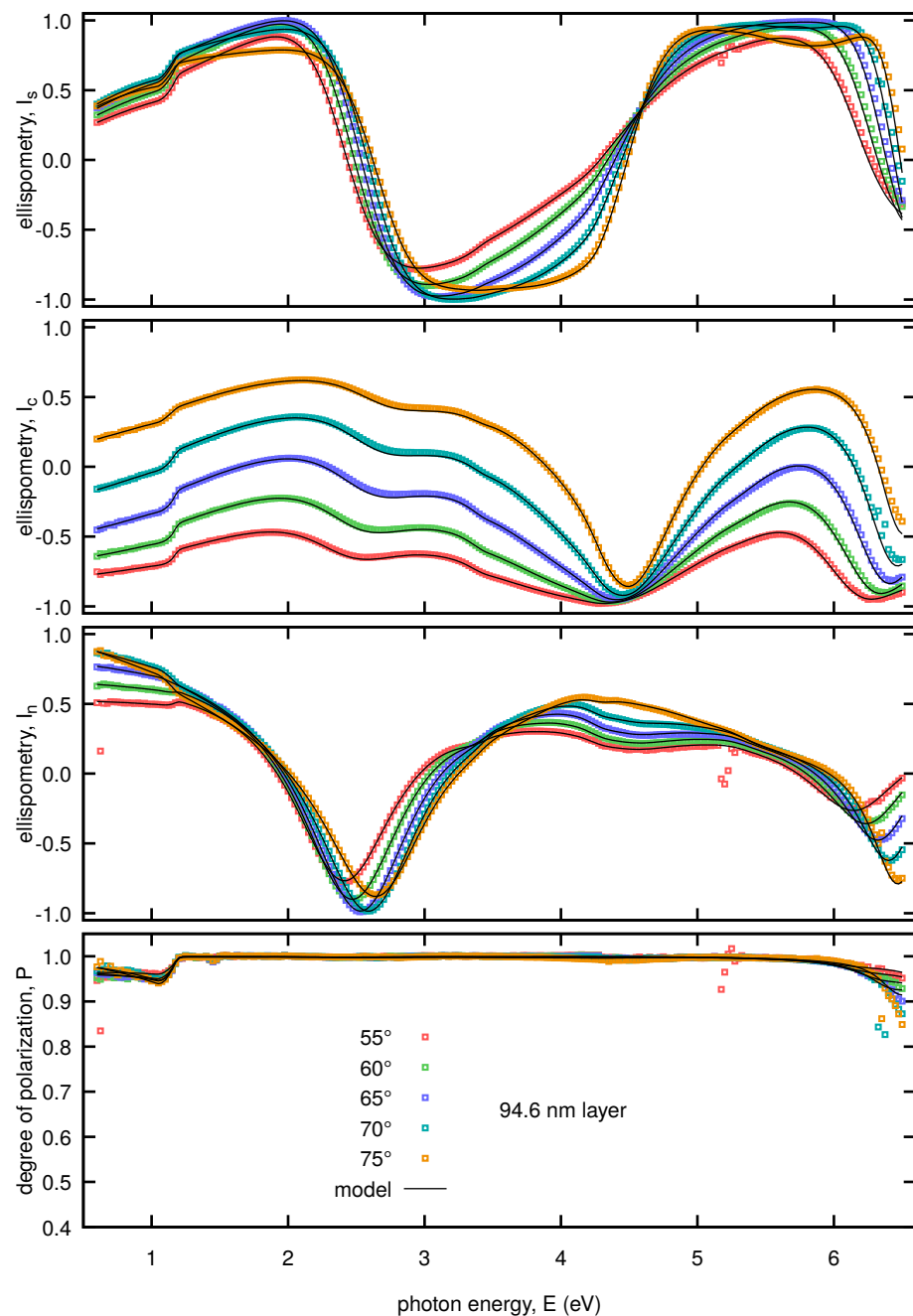


Figure S30. Spectral dependencies of the generalized ellipsometric parameters displayed for the 94.6 nm thick film.

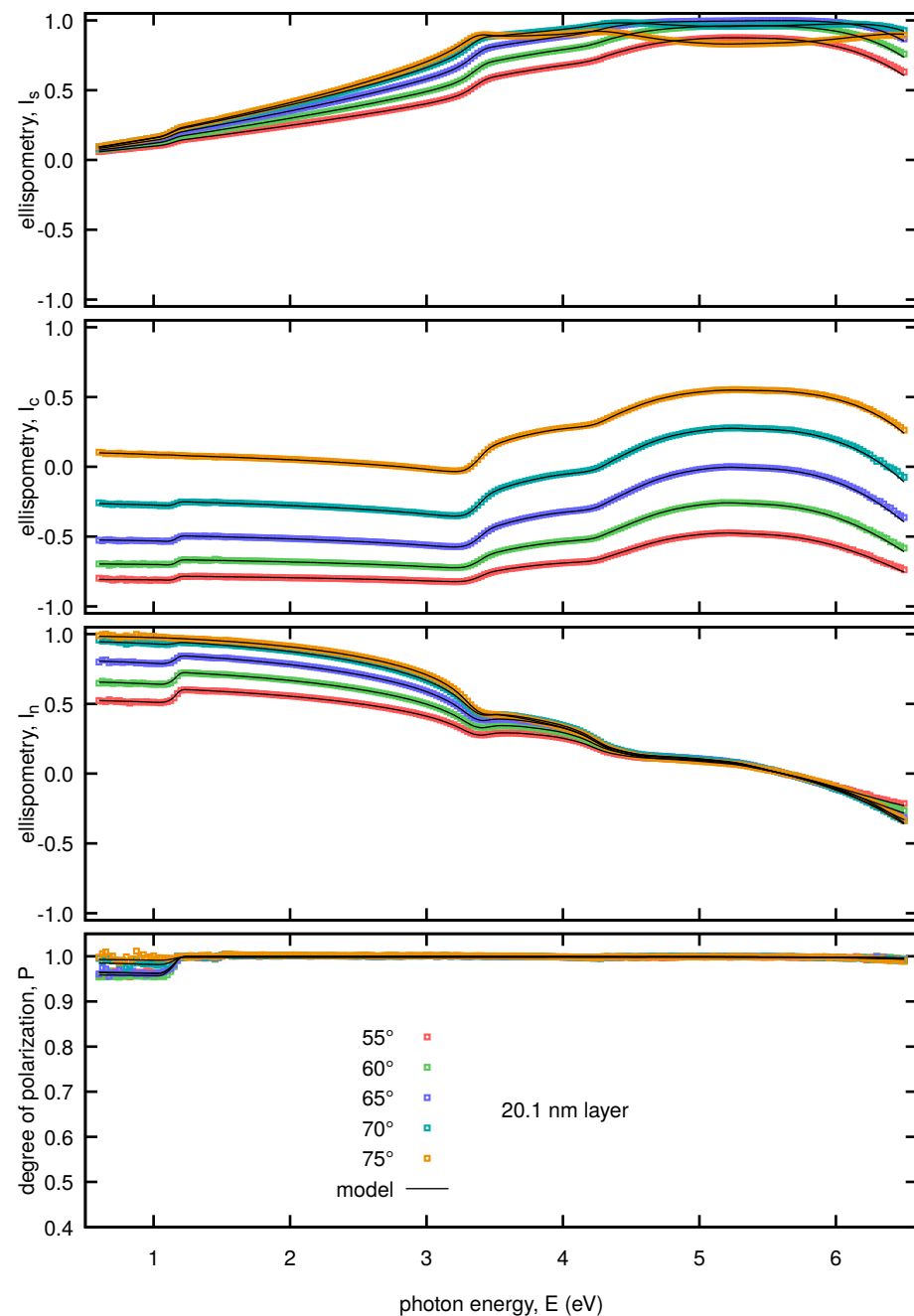


Figure S31. Spectral dependencies of the generalized ellipsometric parameters displayed for the 20.1 nm thick film.

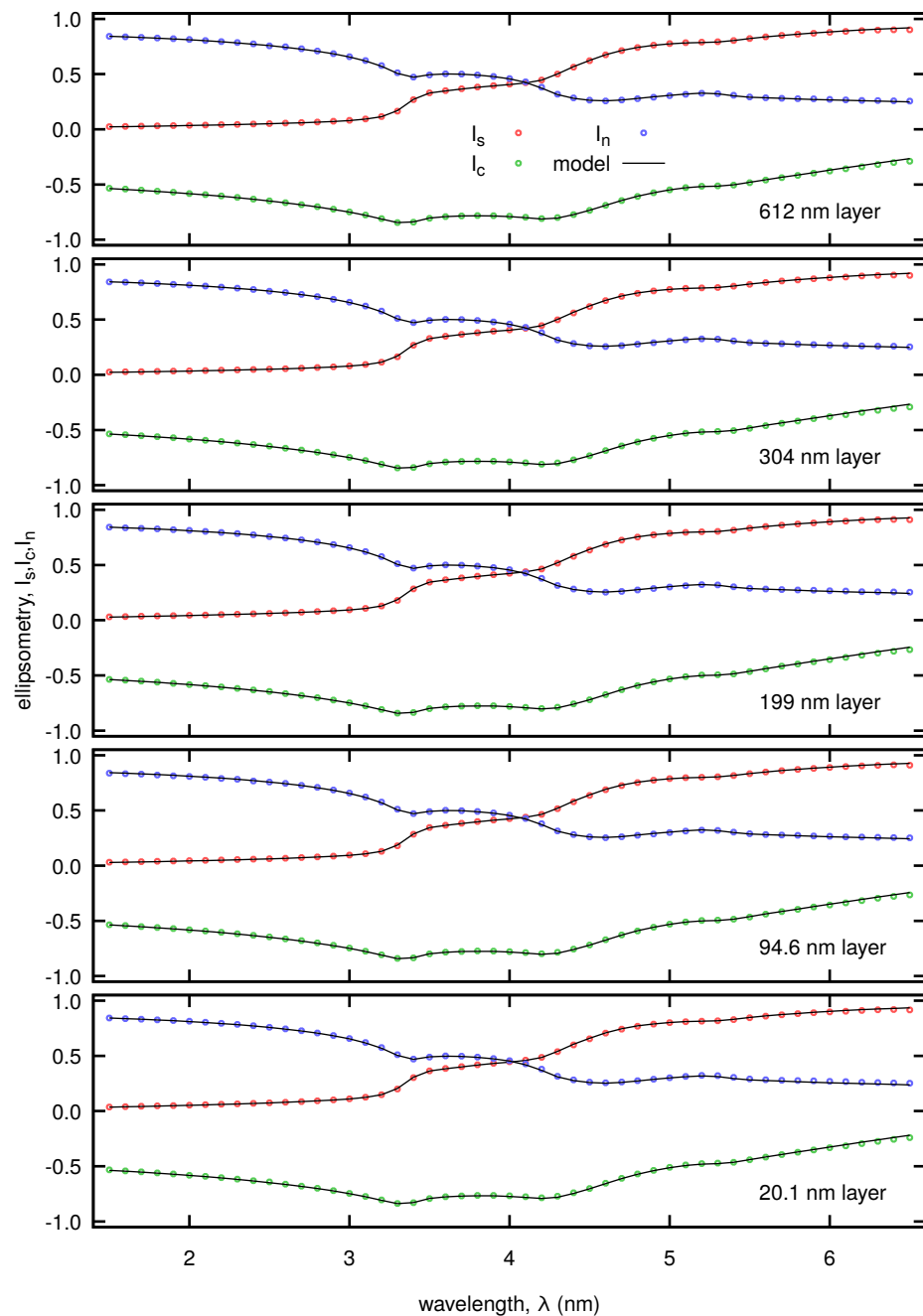


Figure S32. Spectral dependencies of the back side ellipsometry of all the samples.

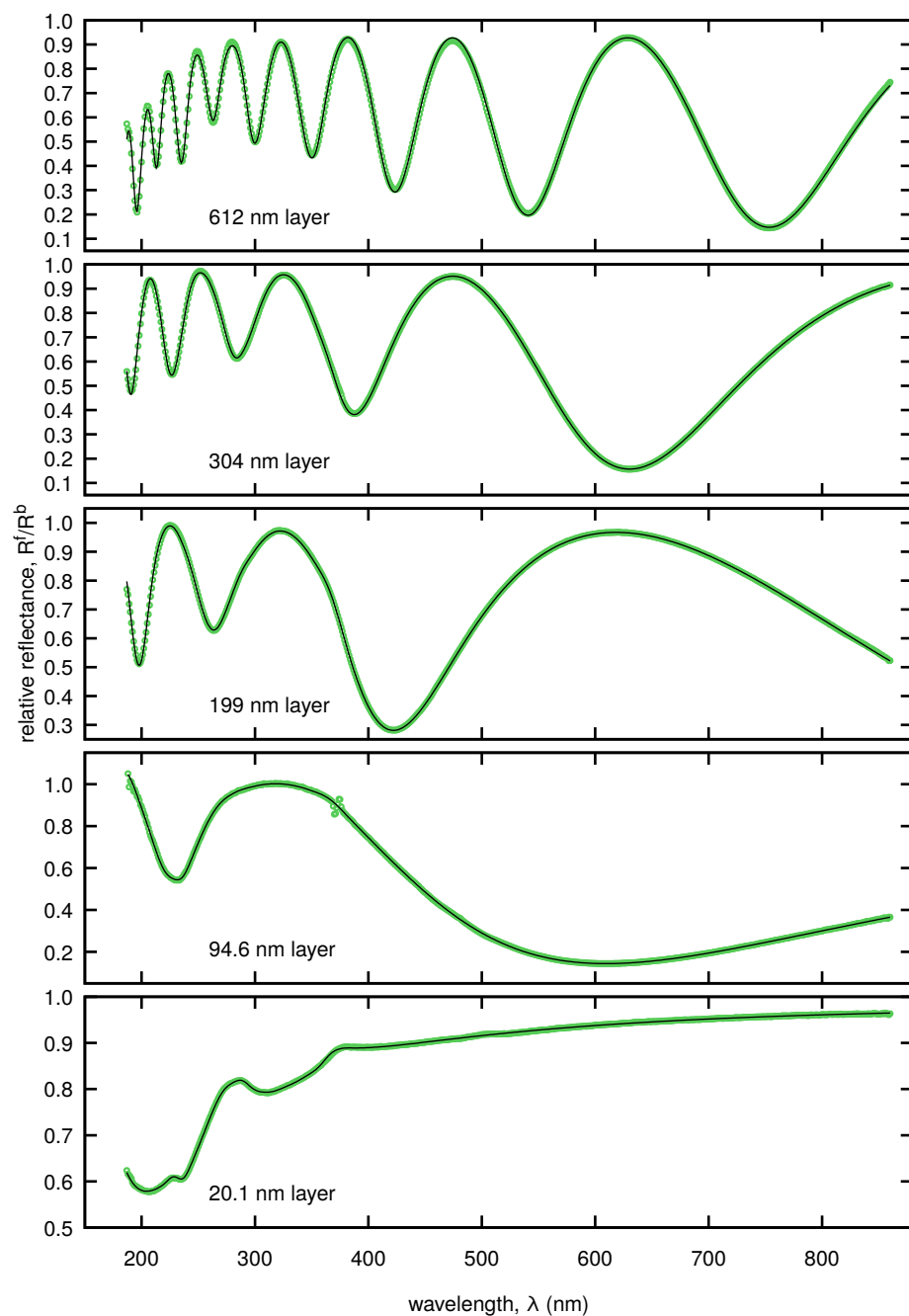


Figure S33. Spectral dependencies of the relative reflectance of all the films.

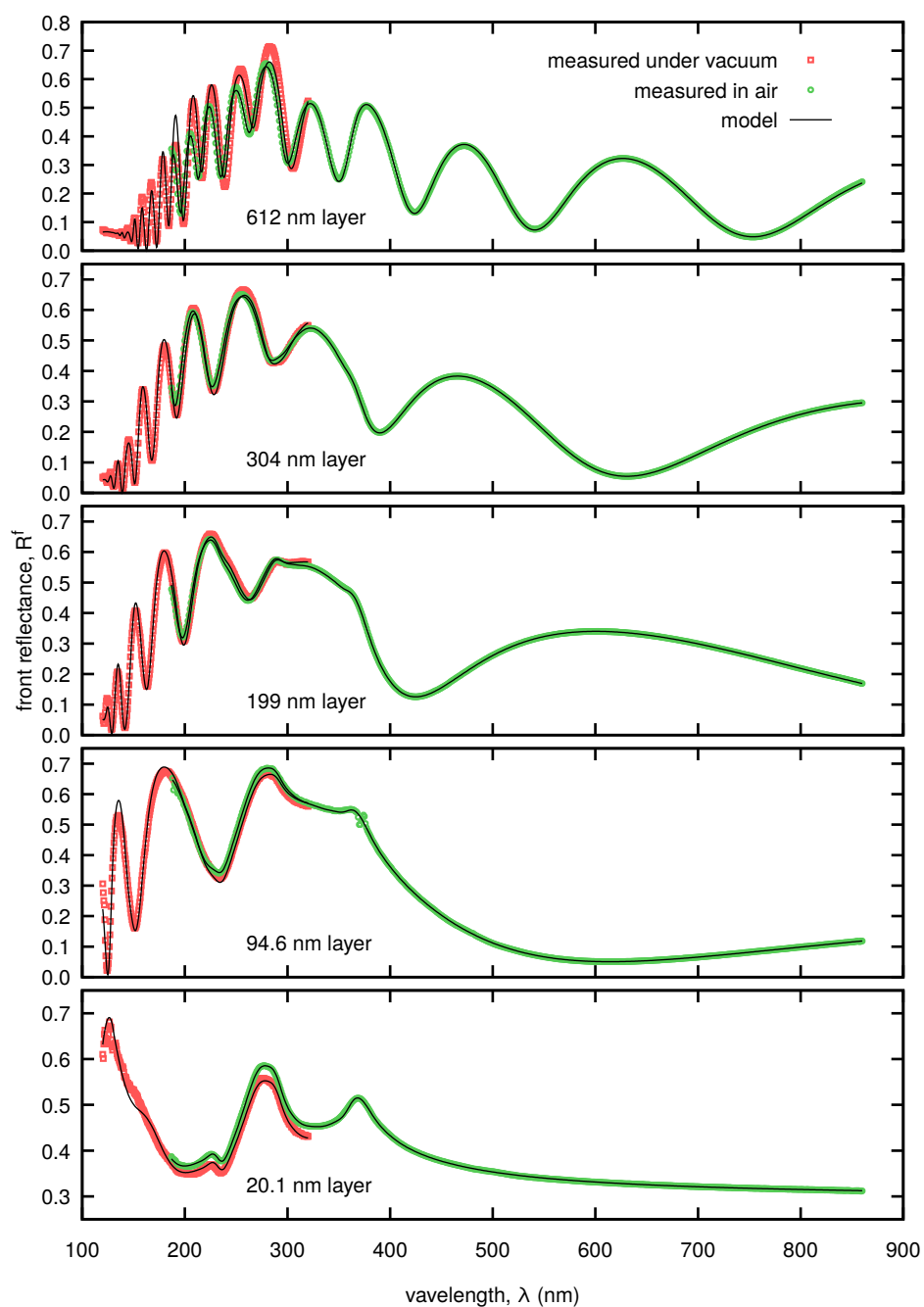


Figure S34. Spectral dependencies of the reflectance of all the films.

2. AFM characterization

AFM topography was measured using Dimension Icon microscope (Bruker), tapping mode and RTESPA-525 tapping mode probes. Scan range was 5x5 micrometers and pixel resolution was 512x512 pixels.

Measurement uncertainty was dominated by tip convolution as the surface consists of very sharp features; every tip produced slightly different topography and tips got worn quickly. A very light tapping mode was used to get a consistent dataset using a single probe. Based on using several new SPM tips and measuring approximately the same area, the estimated uncertainty of the statistical quantities is 25%.

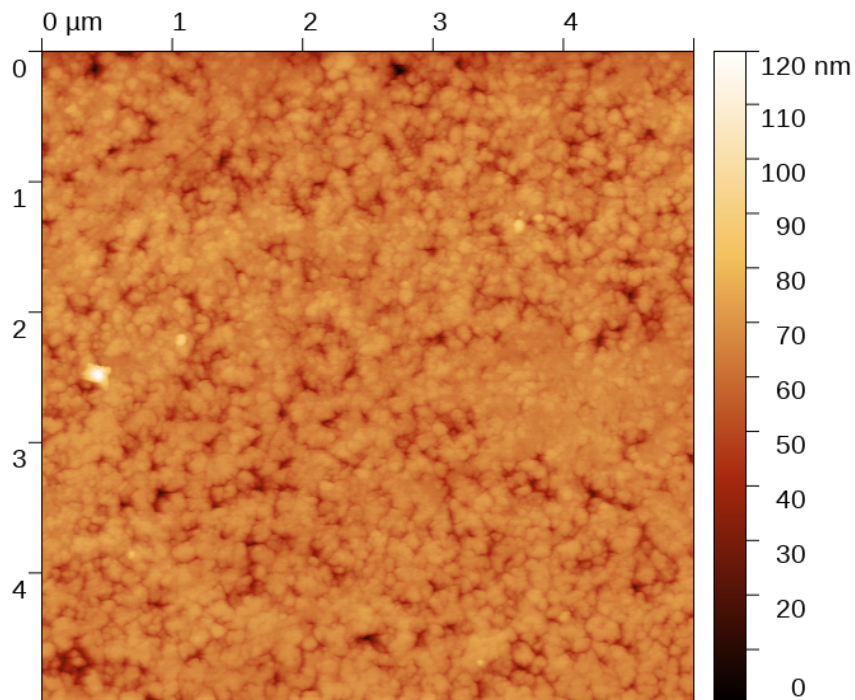


Figure S35. AFM topography of 612 nm thick GdF₃ film (sample #1).

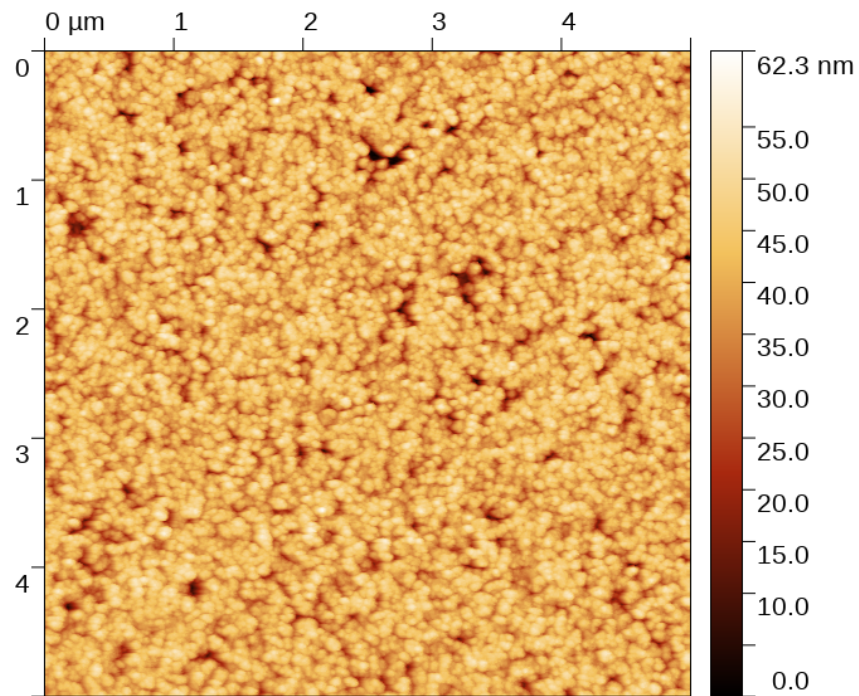


Figure S36. AFM topography of 304 nm thick GdF_3 film (sample #2).

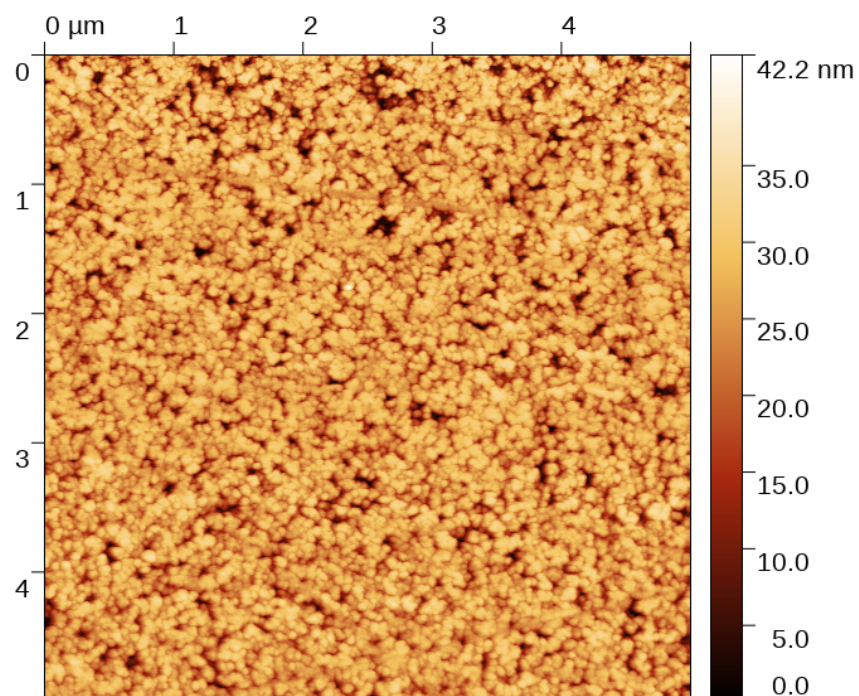


Figure S37. AFM topography of 199 nm thick GdF_3 film (sample #3).

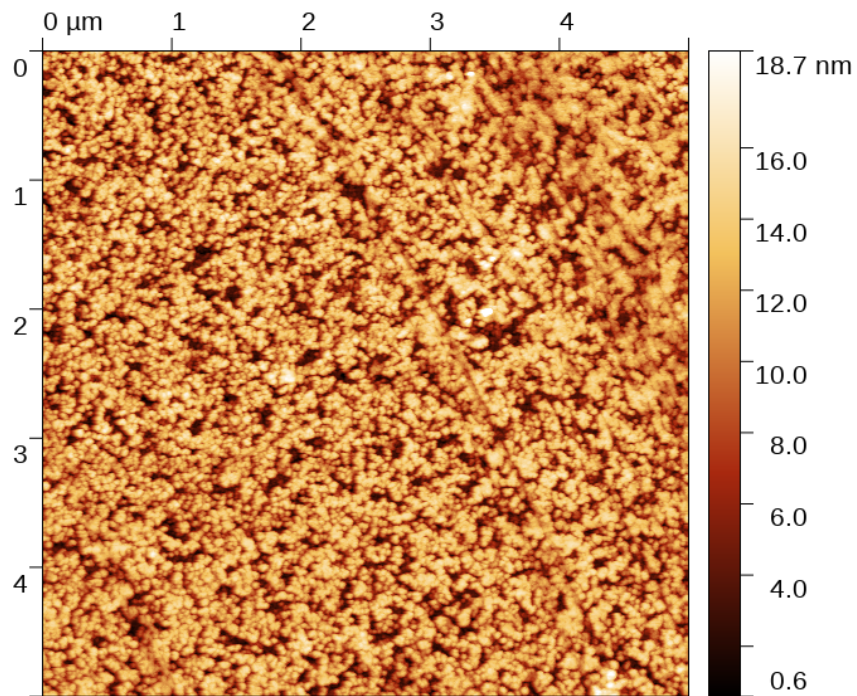


Figure S38. AFM topography of 94.6 nm thick GdF_3 film (sample #4).

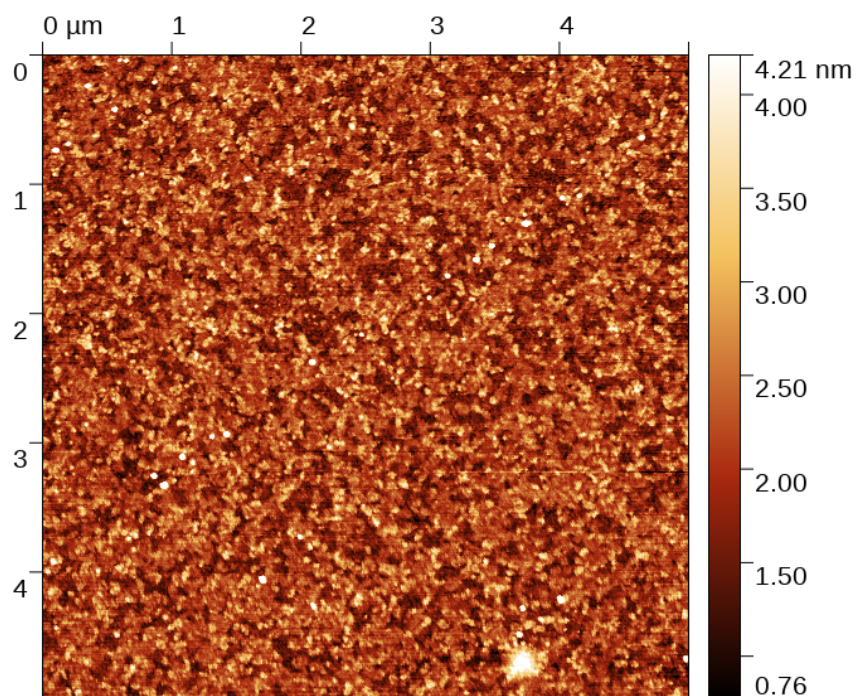


Figure S39. AFM topography of 20.1 nm thick GdF_3 film (sample #5).

3. Penalization function

The sum of squares of differences between experimental and modeled data are completed by penalization functions ensuring positive values of response function ε_i in the following form:

$$S = \sum_j (1 + \exp(-\kappa \varepsilon_i(E_j)))^2,$$

where summation j is performed over the photon energies in the region of interest. In Figure S40 the photon energies where the penalization functions were applied is displayed. The minimization algorithm trying to find such a response functions that the penalization functions are closest to unity. The parameter κ define the strength of the penalization function.

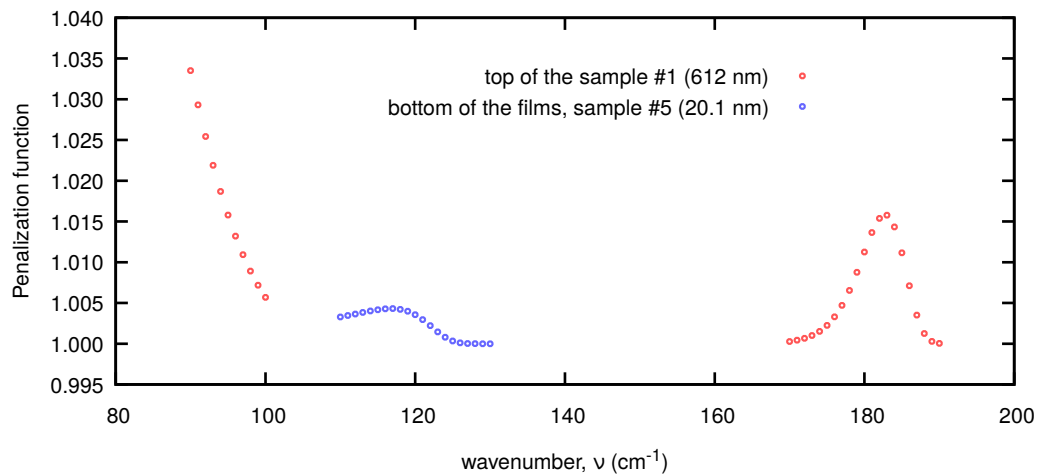


Figure S40. Penalization functions for $\kappa = 10$.

4. Multi-phonon excitations

Table S2. Dispersion parameters of multi-phonon contributions.

		sample			
		#1	#2	#3	#4 & #5
transition strength $N_{\text{ph},10}$ (10^{-3}eV^2)	0.22(6)	0.25(7)	0.25(7)	0.07(4)	
resonant frequency $\nu_{\text{ph},10}$ (cm^{-1})			417.6(11)		
broadening $\beta_{\text{ph},10}$ (cm^{-1})			38(4)		
Lorentzian part $L_{\text{ph},10}$			0.8(2)		
transition strength $N_{\text{ph},11}$ (10^{-3}eV^2)	0.107(15)	0.065(10)	0.025(7)	0.020(4)	
resonant frequency $\nu_{\text{ph},11}$ (cm^{-1})			473.0(4)		
broadening $\beta_{\text{ph},11}$ (cm^{-1})			33.6(12)		
Lorentzian part $L_{\text{ph},11}$			0.0(2)		

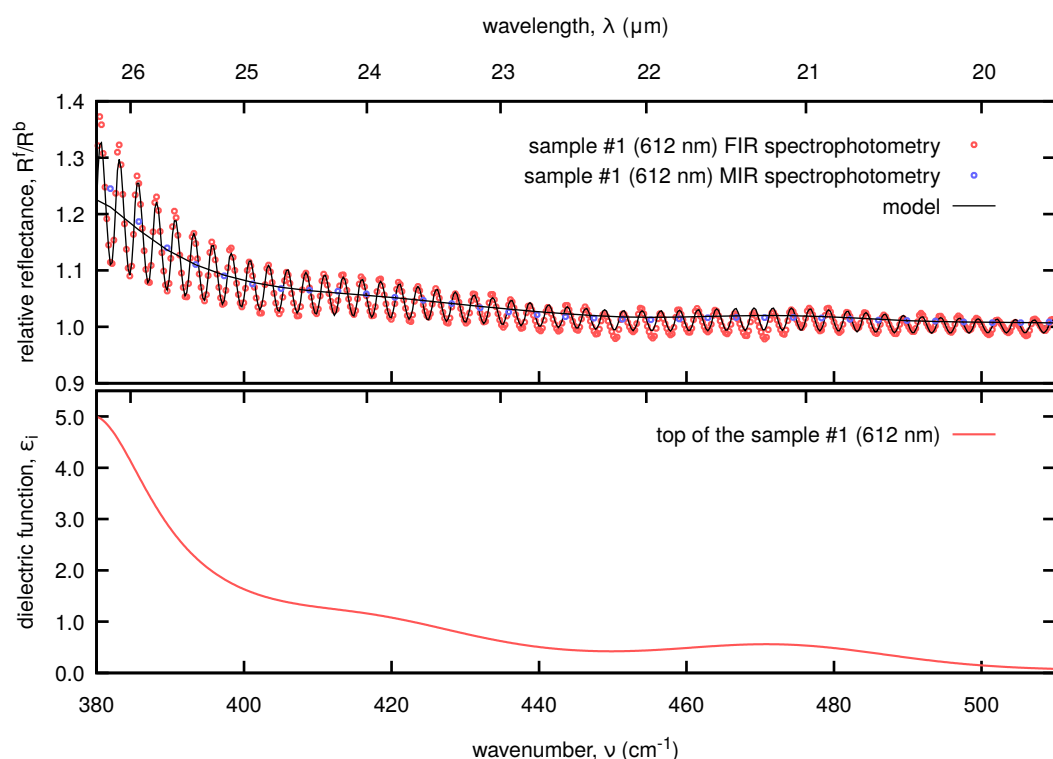


Figure S41. Spectral dependence of the FIR and MIR relative reflectances (the ratio of front and back reflectance) in multi-phonon region displayed for chosen GdF_3 film (top panel) and spectral dependencies of the imaginary part of dielectric functions on the top the film (bottom panel).

5. Optical constants – GdF₃-Enk.txt, Si-FZ-Enk.txt, Si-NOL-Enk.txt

The optical constants of the GdF₃, float zone silicon and silicon native oxide layer determined and used in our study are presented in Figs. S42, S43 and S44. In file **GdF3-Enk.txt** the optical constants corresponding to the bottom of the films are generated, *i.e.* GdF₃ host material without adsorbed components. These optical constants are the best description of very thin film (in order of tens of nanometers) used in interference systems. In files **Si-FZ-Enk.txt** and **Si-NOL-Enk.txt** are generated room temperature optical constants of float zone silicon and native oxide layer used in our study. The optical constants are modeled also using the UDM with the parameters obtained in our previous works cited in the main article.

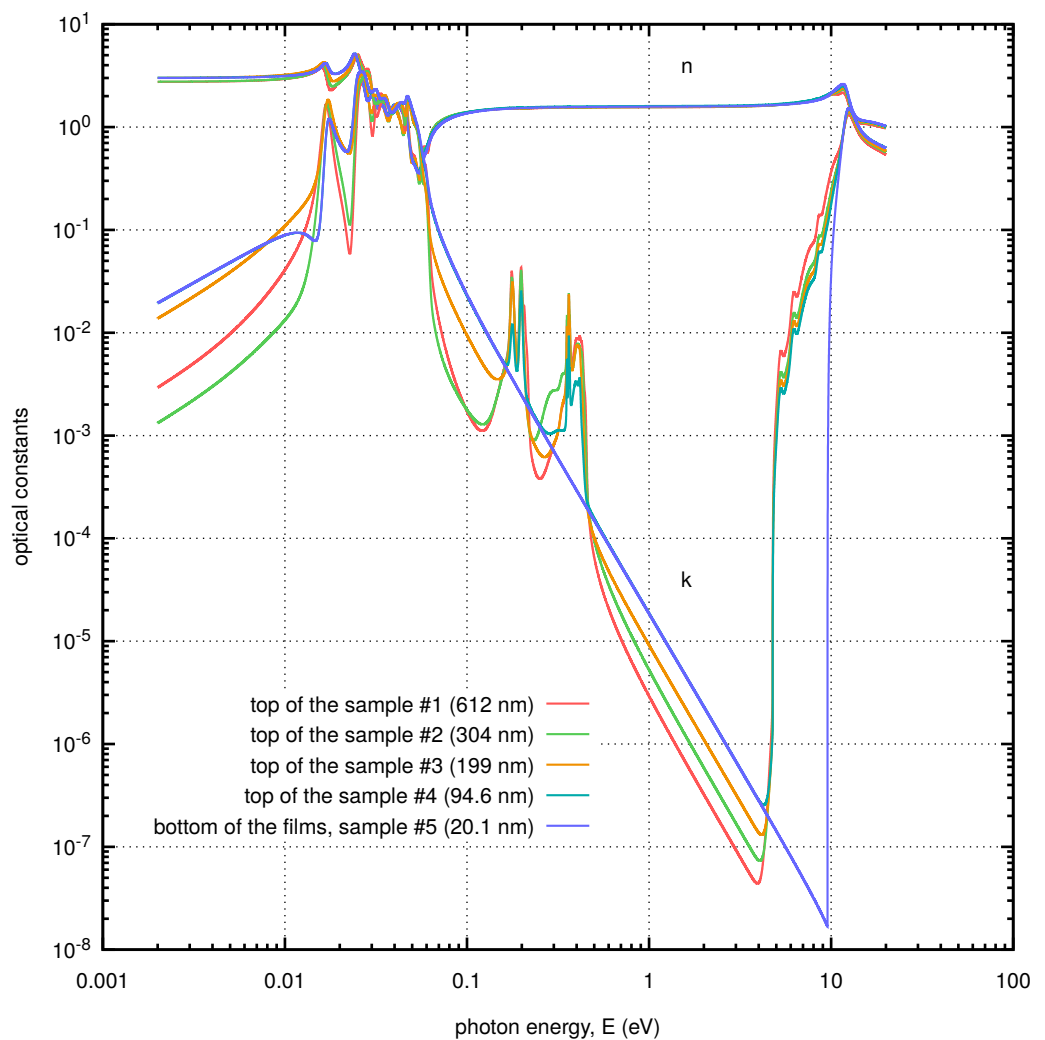


Figure S42. The plot of GdF₃ optical constants.

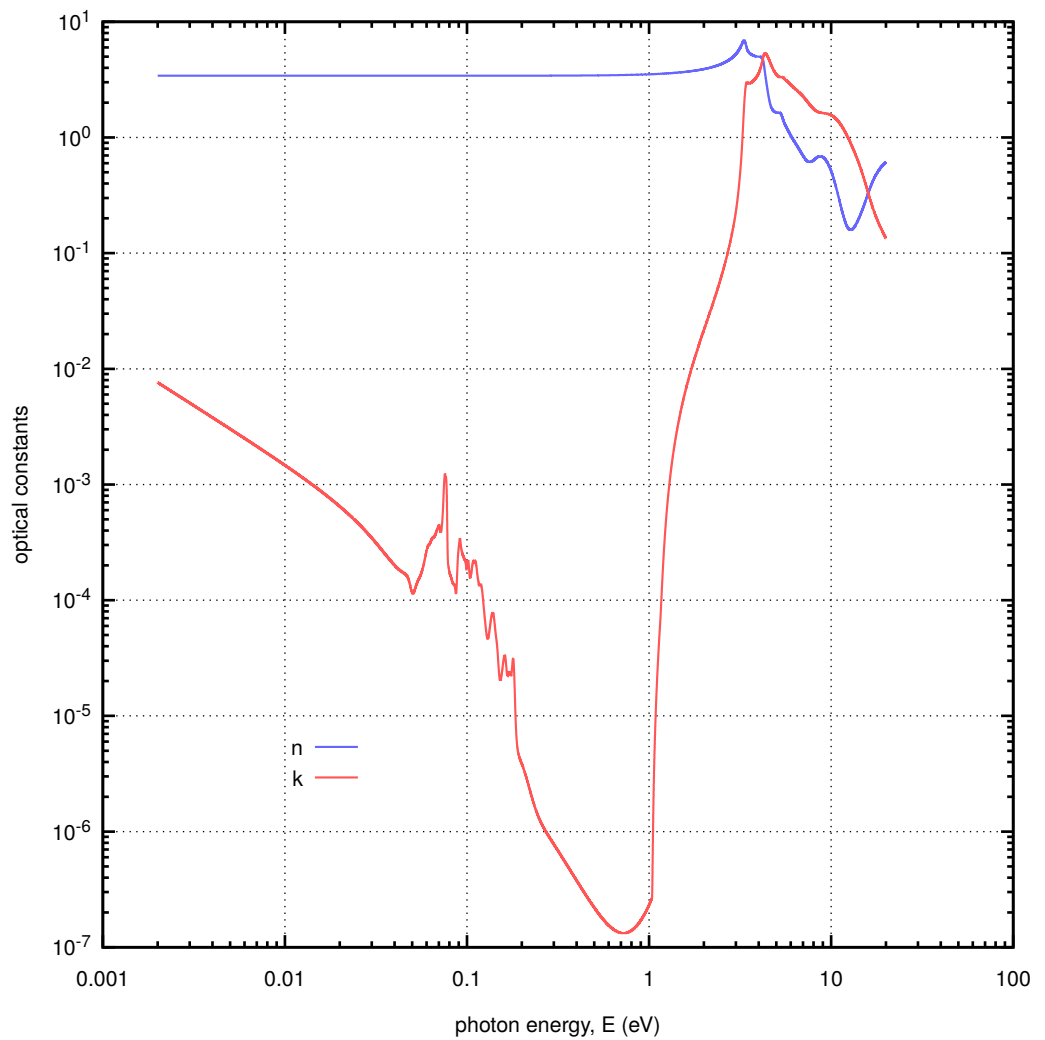


Figure S43. The plot of float zone silicon optical constants.

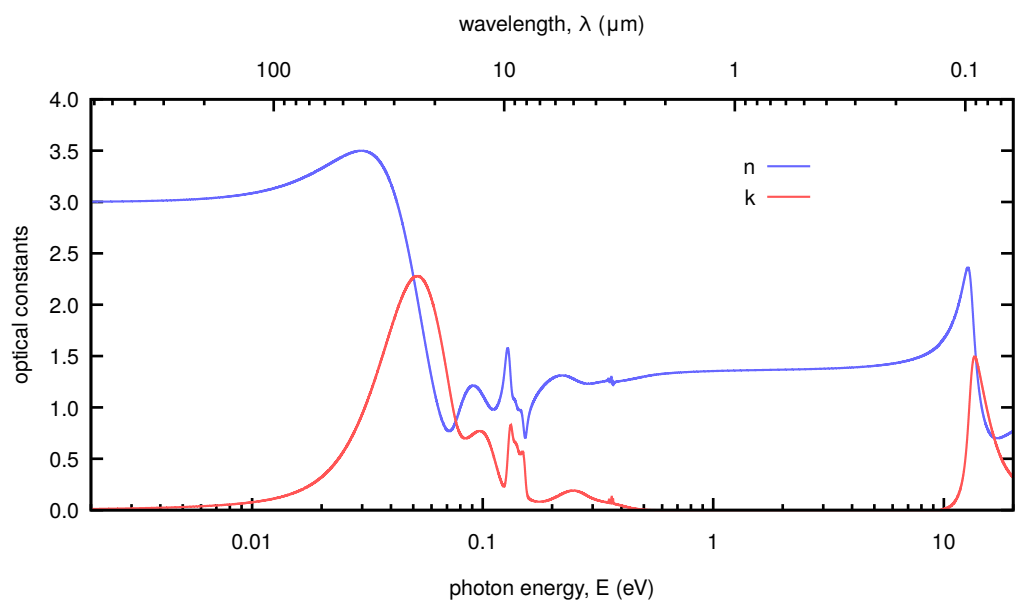


Figure S44. The plot of silicon NOL optical constants.